ChemComm

Going for Gold – The Chemistry of Structurally Authenticated Gold(I)-Ethylene Complexes

Journal:	*ChemComm*
Manuscript ID	CC-FEA-02-2024-000676.R1
Article Type:	Feature Article

Going for Gold – The Chemistry of Structurally Authenticated Gold(I)-Ethylene Complexes

Brandon T. Watson and H. V. Rasika Dias*

Department of Chemistry and Biochemistry, The University of Texas at Arlington, Arlington, Texas 76019, United States

*Correspondence to: dias@uta.edu

Abstract

Gold coordination chemistry and catalysis involving unsaturated hydrocarbons such as olefins have experienced a remarkable growth during the last few decades. Despite the importance, isolable and well-characterized molecules with ethylene, the simplest and the most widely produced olefin, on gold are still limited. This review aims to cover features of, and strategies utilized to stabilize gold-ethylene complexes and their diverse use in chemical transformations and homogeneous catalytic processes. Isolable and well-authenticated gold-ethylene complexes are important not only for structural, spectroscopic, and bonding studies but also as models for

likely intermediates in gold mediated reactions of alkenes and gold-alkene species observed in gas phase. There has also been development on $Au^{I/III}$ catalytic cycles. Nitrogen based ligands have been the most widely utilized ligand supports thus far for the successful stabilization of gold-ethylene adducts. Gold has a bright future in olefin chemistry and with ethylene.

Introduction

For nearly all human history, gold has been considered as an unreactive or noble metal with no utility outside of decorations and accumulating wealth. However, as a result of scientific ingenuity and several groundbreaking efforts, the field of gold chemistry, and in particular catalysis and organometallic chemistry of gold involving alkenes have completely been revolutionized in the last few decades.[1-15] Early work indicated that although bulk gold is rather inert, gold on the nano-scale is quite reactive and useful in mediating chemical transformations.[16, 17] Although there were scattered reports on the use of gold in heterogeneous catalysis, including gold-catalyzed oxidative acetoxylation of ethylene to vinyl acetate,[18] the true potential of gold on the nano-scale for catalysis was not appreciated until the ground breaking work by Bond and Sermon on hydrogenation of olefins,[19, 20] as well as by Hutchings on hydrochlorination of acetylene[21] and Haruta *et al.* on low temperature oxidation of CO.[22-27] More relevant to smaller alkenes, Haruta and co-workers found that gold is also an excellent catalyst for the epoxidation of propylene to propylene oxide, a useful C3 synthon.[12, 28, 29] Guzman and Gates demonstrated that $[Au^{III}(CH_3)_2(acac)]$ supported on magnesium oxide is a competent catalyst for the hydrogenation of ethylene.[30, 31]

In 1986, Ito and Hayashi reported the first application of gold(I) in homogeneous catalysis.[32] Afterwards, early work was done utilizing gold(I) to activate alkynes towards nucleophilic addition of traditionally weak nucleophiles such as methanol[33] and water,[34] circumventing the need for toxic mercury(II) compounds. Until more recently, the role of gold in the homogeneous catalysis of unsaturated hydrocarbons was limited to alkynes.[35] In 2000, Hashmi *et al.* reported a gold(III) catalyzed addition of a hydroxy group to an activated alkene, as well as the hydroarylation of an enone (methyl vinyl ketone) with 2-methylfuran.[36] Kobayashi *et al.* would later utilize $AuCl_3$ for the Lewis acid-catalyzed hydroamination of various enones with carbamates.[37] Toste and co-workers reported a stereoselective alkene cyclopropanation with propargyl acetate using $PPh_3AuCl/AgSbF_6$ in 2005.[38] Gold(I)-catalyzed hydroamination of alkenes has also been reported by Che in 2006 using sulfonamides[39] and He in 2006 using benzyl carbamate.[40] He and Yang reported the gold(I)-catalyzed hydroalkoxyation of 4-phenylbutene with phenol in 2005.[41] Cinellu *et al*. utilized a dimeric gold(III) oxo complex for the epoxidation of norbornene, with high selectivity for the *exo* product.[42] They also described the spectroscopic data of a Au(I)-ethylene species.[43] Carbene transfer reactions from ethyl diazoacetate mediated by a structurally characterized gold(I) ethylene to saturated and unsaturated hydrocarbons were reported by Flores and Dias.[44] More recently, Tilset and co-workers have observed and studied the 1,2-insertion of ethylene into a Au^{III}-O_2CCF_3 bond.[45] Other processes of ethylene involving gold such as cyclopropanation, hydroamination, oxyarylation, *etc.* are also known.[46-50]

Recently, there has also been work done on Au^{I}/Au^{III} catalytic cycles, analogous to traditional Pd^{0}/Pd^{II} cycles. Previously considered unlikely due to many challenges such as higher oxidation potential (*i.e.,* E°_{red} $Au^{III/I}$ = 1.41 V, E°_{red} $Pd^{II/0}$ = 0.92 V, E°_{red} $Pt^{II/0}$ = 1.18 V which is

isoelectronic with $Au^{III/I}$)[51-53] and the instability of Au^{III} intermediates, which has long impeded the development of Au^{I}/Au^{III} catalysis.[54, 55] Initial work was done involving strategies such as the addition of strong external oxidants (*e.g.,* F^+ sources or hypervalent iodanes),[56, 57] and later accomplished by light, thermal, or base activation.[58-64] Through clever ligand design,[65, 66] specifically through the use of chelating ligands that enforce bending at gold(I) affecting its electronic properties,[15] it is now possible to accomplish oxidative addition of iodoarenes without the need of external oxidants and with mild conditions, enabling the development Au^{I}/Au^{III} catalytic cycles, which will be highlighted later in this review.

Overall, there is a growing number of literature reports and excellent reviews on gold mediated chemistry.[4, 6, 11] Despite the importance and great utility of gold(I) in numerous transformations of unsaturated hydrocarbons, very few structurally authenticated gold(I)-(π-ligand) complexes are available in the literature, particularly with the simplest π-ligand, and the organic chemical produced in largest quantities worldwide, ethylene.[67, 68] They are important not only for structural, spectroscopic and bonding studies but also as models for likely intermediates in gold mediated reactions of alkenes in homogeneous and heterogeneous processes, and gold-alkene species observed in gas phase.[69, 70] At the time of writing our previous review in 2008 on coinage metal ethylene complexes,[71, 72] there were only 3 structurally characterized gold(I)-ethylene complexes in the literature. Since then, this number has grown to 25 complexes,[73] comprised of 10 neutral complexes and 15 cationic complexes. They are quite difficult to stabilize partly due to entropic factors associated with fixing a gas. This review aims to describe the developments of coordination and organometallic chemistry of gold involving ethylene with the specific focus on the well-defined, structurally characterized gold-ethylene

complexes, and to examine trends across different ligand systems, and serve as a useful resource for future work. This review will occasionally refer to complexes using their Cambridge Structural Database (CSD) Refcode.[73]

Gold(I)-Ethylene Bonding

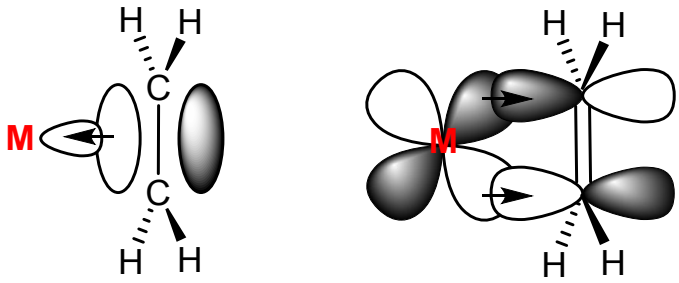

Figure 1. Dewar-Chatt-Duncanson model, σ-donation from π-orbital of ethylene to vacant orbital of the metal (left) and π-backdonation from a filled metal d-orbital to the vacant π* antibonding orbital of ethylene (right).

The bonding in metal-olefin complexes is comprised of a mixture of electrostatic interactions, as well as a synergistic combination of σ-donation from the π-ligand and π-backdonation from the metal to the π* antibonding orbital, as per the Dewar–Chatt–Duncanson model (Figure 1).[74, 75] The nature of interaction between the group 11 (coinage) metals and ethylene was a focus for a number of years by several groups.[76-80] Recent computational and spectroscopic data suggest that among the coinage metals (copper, silver, and gold), the interaction energy is usually the greatest for gold and least for silver, and that there is a substantial metal-olefin π-backbonding component in gold, notably in their neutral complexes.[43, 71, 78, 81-84] This trend is also observed among group 10 metals, in which the 5d metal Pt(II) displays the greatest metal-ethylene interaction and the 4d metal Pd(II) displays the weakest interaction, with the 3d metal Ni(II) having an intermediate strength interaction.[85] The extent of π-

backdonation and thus the strength of the metal-ethylene interaction can be gauged by a lengthening of the C=C bond using X-ray diffraction (XRD), a redshift of the C=C stretching frequency using vibrational spectroscopy (*i.e.*, specifically Raman spectroscopy), as well as the change in chemical shift of the olefinic protons and olefinic carbons using NMR spectroscopy. In 2022, Dias, Roithová, and co-workers performed a collaborative and systematic study of coinage metal π-ligand complexes to further understand the strength and nature of the metal-(π-ligand) interaction, using the aforementioned techniques in tandem with mass spectrometric and computational methods, which will be discussed in further detail in a later section.[86]

Neutral Gold(I)-Ethylene Complexes

Dias and co-workers in 2007 reported the first isolable and structurally characterized gold-ethylene complexes utilizing highly fluorinated κ^2-hydrotris(3,5-bis(trifluoromethyl)-pyrazolyl)borate (**1**, Figure 2) and κ^2-hydrotris(3-(trifluoromethyl)-5-phenyl-pyrazolyl)borate (**2**, Figure 2) supporting ligands.[87] They were prepared *via* salt metathesis using the sodium salt of the respective ligand and gold(I) chloride under an ethylene atmosphere in good yields (77% (**1**) and 81% (**2**)). Remarkably, both compounds were isolated as stable white solids and do not lose ethylene under reduced pressure. The phenyl substituted complex did not show signs of decomposition after exposure to air and ambient lighting after several days. In both complexes (as well as similar tris(pyrazolyl)borate supported complexes which were later reported), the supporting ligand coordinates in a κ^2-fashion, where one pyrazolyl arm is not coordinated to the metal center. The distance between the nitrogen atom of the non-coordinated pyrazolyl arm and

gold(I) center in **1** is 2.710 Å, which is within the sum of van der Waals radii of Au and N,[88, 89] however, this does not distort the trigonal planar geometry at gold, as the sum of angles (excluding the non-coordinated pyrazolyl arm) at gold are 359.5°. For comparison, the bond distances between Au and N of the coordinated pyrazolyl arms for **1** are 2.221(5) and 2.224(5) Å. Despite this asymmetry in the crystal structure, ^{1}H and ^{19}F NMR analyses show only one set of resonances for the pyrazolyl arms (6.97 (^{1}H), -59.4 and -61.9 (^{19}F), $CDCl_3$), even at -80 °C, which indicates that the coordination environment is fluxional in solution on the NMR time scale. Ethylene coordinates in the typical η^2 fashion, and the ethylene carbon atoms are essentially coplanar with the coordinated nitrogen atoms to maximize orbital overlap and π-backbonding.[90-92] This η^2 and coplanar coordination is observed amongst all trigonal planar gold(I)-ethylene complexes which have been reported at the time of writing. The phenyl substituted **2** was also bubbled with excess ethylene at room temperature, and two sharp resonances were observed at 3.69 ppm (bound ethylene) and 5.39 ppm (free ethylene), which suggests that the gold(I)-ethylene interaction is strong and does not exchange with excess ethylene, which would have been evident by the coalescence and broadening of the ethylene resonances.

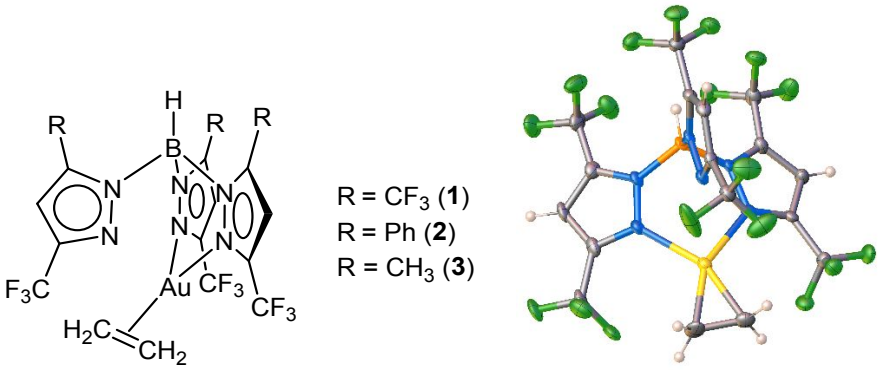

Figure 2. κ^2-[HB(3-(CF_3)-5-(R)-Pz)$_3$]Au(C_2H_4), R = CF_3 (CIMXAY, **1**), R = Ph (CIMXEC, **2**), R = CH_3 (IREBEO, **3**) and a view of the crystal structure (**1**).

Later in 2016,[93] Ridlen *et al.* reported the methyl/trifluoromethyl substituted analog κ^2-hydrotris(3-(trifluoromethyl)-5-methyl-pyrazolyl)borate gold(I)-ethylene (**3**, Figure 2), in a similar manner following (**1**) and (**2**) by reaction of the sodium salt of the ligand with AuCl under an ethylene atmosphere in 80% yield. The complex exhibited similar structural (*i.e.*, κ^2-coordination, trigonal planar geometry, one non-coordinating pyrazolyl arm) and spectroscopic properties to the previous two, as well as similar thermal stability. Solid samples of **3** do not lose ethylene under reduced pressure. X-ray analysis of **3** reveals that it (along with the copper and silver complexes, CSD reference codes IRAZUY and IREBAK respectively) crystallizes in the $P\overline{3}$ space group, with a crystallographically imposed three-fold axis of symmetry along the B-H bond. The Au(C_2H_4) moiety is disordered over three symmetry related sites with equal occupancy. Therefore, the bond distances and angles of **3** associated with the ethylene group should be treated with caution.

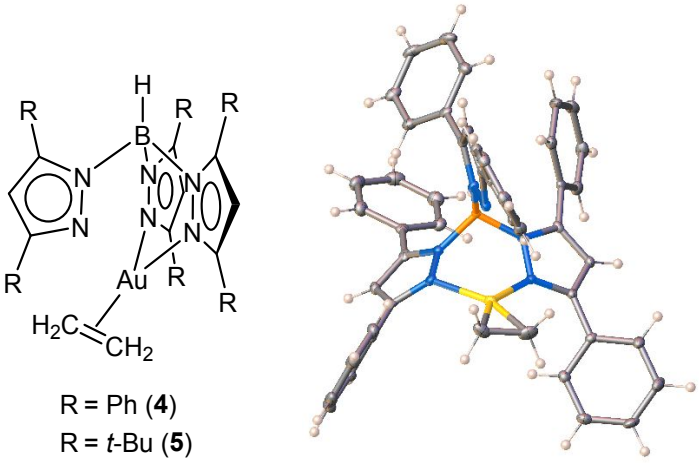

Figure 3. κ^2-[HB(3,5-(R)$_2$-Pz)$_3$]Au(C_2H_4) R = Ph (OKOQEN, **4**), R = *t*-Bu (OKOQIR, **5**), and a view of the crystal structure (**4**).

More recently, in 2021,[83] Wu *et al.* would use the comparably electron-rich tris(pyrazolyl)borate ligands, κ^2-hydrotris(3,5-diphenyl-pyrazolyl)borate and κ^2-hydrotris(3,5-di(*t*-butyl)-pyrazolyl)borate (**4** and **5** respectively, Figure 3) to isolate two highly-unstable gold(I)-ethylene complexes in yields of 77% and 62% respectively. Compared to the three complexes mentioned previously, which feature the electron-withdrawing trifluoromethyl group near the metal center, yielding good thermal stability, these two complexes were highly reactive. Neither complex was stable at room temperature in solution, especially in halogenated solvents, for prolonged periods. The di-*tert*-butyl substituted complex **5** decomposed rapidly in chloroform, and the diphenyl complex **4** shows approximately 30% decomposition in CD_2Cl_2 after 12 hours based on ^{1}H NMR data. Likely due to the electron-rich nature of the supporting ligands, these two complexes display long C=C bonds amongst group-11 ethylene complexes, having C=C bond lengths of 1.413(7) and 1.410(5) Å for **4** and **5** respectively. Additionally, these two complexes exhibit the largest upfield shifts from free ethylene in their ^{13}C NMR of all group-11 ethylene complexes of 67.9 and 66.0 ppm for **4** and **5** respectively. Interestingly, the olefinic protons of ethylene in the di-*tert*-butyl complex **5** resolve into an AA'BB' pattern in the ^{1}H NMR in cyclohexane-d_{12} and toluene-d_8, both at room temperature and at -20 °C, likely due to a large rotational barrier caused by the flanking *tert*-butyl groups.

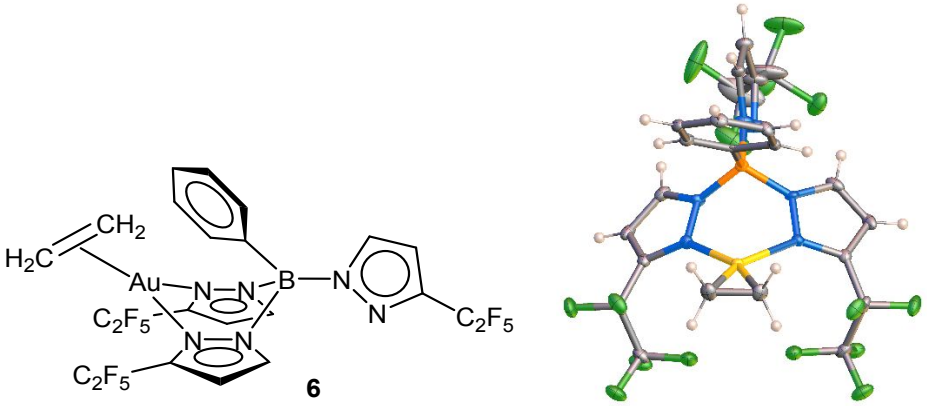

Figure 4. κ^2-[PhB(3-(C_2F_5)-Pz)$_3$]Au(C_2H_4) (BECCIX, **6**) and a view of the crystal structure.

In 2012, Dias group made an effort to prepare the first isostructural series of coinage metal-ethylene complexes (not including the cationic metal-tris(ethylene) complexes) by utilizing a B-phenyl substituted phenyltris(3-(pentafluoroethyl)-pyrazolyl)borate ligand (**6**, Figure 4).[94] With this ligand, Dias and Wu were able to isolate the copper(I), silver(I), and gold(I)-ethylene complexes, in which the tris(pyrazolyl)borate ligand in all three complexes coordinates through only two of the pyrazolyl arms with the phenyl group sitting above the metal. The gold(I) complex (**6**) was isolated in 77% yield. Unlike the previous tris(pyrazolyl)borate supported gold(I) complexes which have the non-coordinated pyrazole arm in close contact to the metal center, the B-phenyl substituted complexes have the non-coordinated pyrazole arm residing away from the metal center, suggesting that having the phenyl group sitting above the metal is favorable. This would also be observed later with B-phenyl substituted tris(pyridyl)borate complexes.[84, 95, 96] Despite the clear difference in coordinating and non-coordinating pyrazole arms in the crystal structure, only one set of resonances was observed in the ^{1}H, ^{13}C{^{1}H}, and ^{19}F NMR for the copper, silver, and gold complexes at room temperature, which is in agreement with the coordinational

fluxionality of the donor arms of the tris(pyrazolyl)borate ligand in solution afforded by the flexibility of the tetrahedral boron linkage.

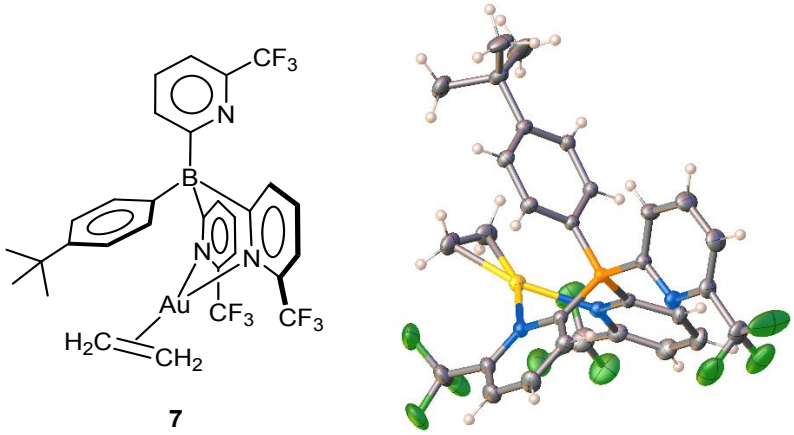

7

Figure 5. κ^2-[(4-*t*-BuC_6H_4)B(6-(CF_3)-Py)$_3$]Au(C_2H_4) (FARTOL, **7**) and a view of the crystal structure.

Based on the experience with tris(pyrazolyl)borates as well as Jäkle's introduction of the tris(pyridyl)borates to the scorpionate family in 2012,[97] the Dias group sought to prepare a fluorinated tris(pyridyl)borate ligand and its coinage metal-ethylene complexes. In 2022, Vanga *et al.* reported the first tris(pyridyl)borate ligand bearing a substituent at position 6 of the pyridyl ring from the reaction of isolated 6-(trifluoromethyl)-2-pyridylmagnesium chloride with dibromo(4-*tert*-butylphenyl)borane in 86% yield,[84] and utilized it to prepare an isostructural series of coinage metal-ethylene complexes which includes a gold(I) complex with an isolated yield of 62%. These complexes do not lose ethylene under reduced pressure. Despite previous metal complexes (Fe, Ru, Mn, V, Zn, Ca, Mg, Ni)[97-103] supported by phenyltris(pyridyl)borate

ligands featuring the expected κ^3 coordination, all three coinage metal complexes (*e.g.,* **7**, Figure 5) featured κ^2 coordination, with the third pyridyl group pointed away from the metal and the phenyl group sitting over the metal, similar to the phenyltris(pyrazolyl)borate complexes (**6**, Figure 4). Interestingly, based on room temperature NMR, the copper complex displayed well resolved resonances for the coordinated/non-coordinated pyridyl arms, suggesting slow interconversion between κ^2 and κ^3 modes on the NMR time scale, whereas the silver complex displayed one set of averaged resonances suggesting fast interconversion, with the gold having partially resolved resonances. Computational studies were also done, where it was determined that the κ^2 conformation for this ligand was more stable than the κ^3 conformation by 13.7, 13.6, and 21.6 kcal mol^{-1} for Cu, Ag, and Au respectively. Further studies were done to analyze the metal-ethylene interaction, and for the gold-ethylene complex 60.4% of the interaction can be attributed to electrostatic interactions, 36.0% to orbital stabilization/covalency, and 3.6% to London type interactions. Additionally, of the orbital interactions, π-backbonding (49.6%) dominates σ-donation (36.2%) for the gold-ethylene complex.

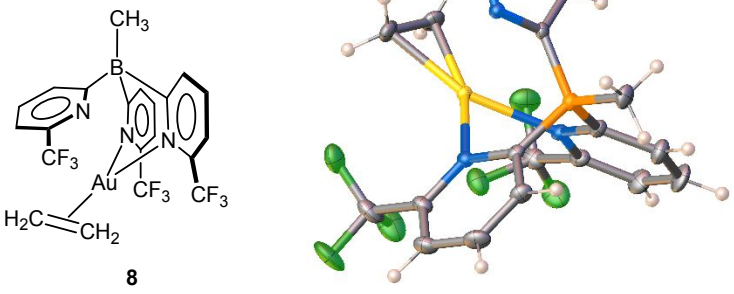

8

Figure 6. κ^2-[CH_3B(6-(CF_3)-Py)$_3$]Au(C_2H_4) (GIBYAV, **8**) and a view of the crystal structure.

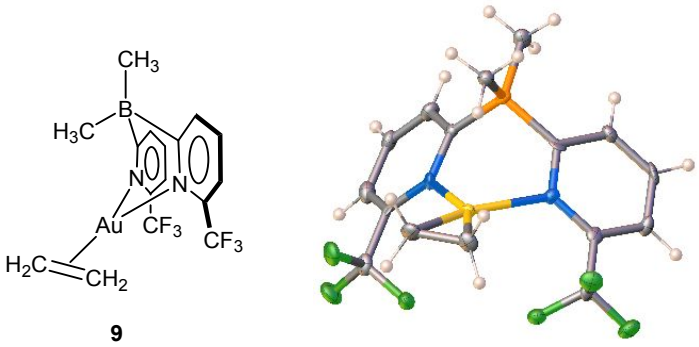

9

Figure 7. κ^2-[$(CH_3)_2$B(6-(CF_3)-Py)$_2$]Au(C_2H_4) (GIBXIC, **9**) and a view of the crystal structure.

In addition to the molecules involving the B-phenyl substituted poly(pyridyl)borates ((4-(*t*-butyl)phenyl)tris(6-(trifluoromethyl)-2-pyridyl)borate and diphenylbis(6-(trifluoromethyl)-2-pyridyl)borate) in 2022,[96] the B-methyl substituted poly(pyridyl)borates have been investigated by Watson and Vanga of the same group to compare the effect of changing the B substituent (from phenyl to methyl) as well as to probe the interplay between κ^3/κ^2 complexes. The B-methylated poly(pyridyl)borate ligands bearing substituents at the 6-position of pyridine,[104] methyltris(6-(trifluoromethyl)-2-pyridyl)borate and dimethylbis(6-(trifluoromethyl)-2-pyridyl)borate have been prepared in a similar method to their previous ligands, by the reaction of 6-trifluoromethyl-2-pyridylmagnesium chloride with tetra(*n*-butyl) ammonium methyltrifluoroborate and bromo(dimethyl)borane in 51% and 90% yields respectively. The utilization of bench stable methyltrifluoroborate salts (potassium and tetra(*n*-butyl) ammonium) greatly simplified the ligand synthesis, as compared to previous reports using air sensitive aryl(dihalo)boranes and diaryl(halo)boranes. These ligands would be utilized to prepare two series of coinage metal-ethylene complexes. The complexes of interest, (**8** and **9**) were prepared in 67% and 88% yields respectively. Both of these gold(I) complexes (**8** and **9**) are quite stable

under nitrogen at -20 °C in solution and as solids, but they do decompose within 1 hour at room temperature. Likely due to steric interactions of the trifluoromethyl groups with ethylene, the tris(pyridyl)complexes (*i.e.,* **8**, Figure 6) adopted a κ^2 coordination mode with one pyridyl arm twisted to be almost parallel to the metal-ethylene plane, but the coordinated/non-coordinated pyridyl rings are highly fluxional in solution based on NMR data. In the bis(pyridyl)borate complex (**9**, Figure 7), the Au•••CH_3B distance is 3.09 Å (average of two molecules in the asymmetric unit), however there is no observable agostic interaction effect, as the sum of all angles about the gold center (not including the CH_3B group) is 359.93° (*av.*). Despite the asymmetry of the two methyl groups in the crystal structure, there is only one observable resonance in the room temperature ^1H and ^{13}C NMR data, suggesting fast ring inversion on the NMR time scale which is consistent with similar rhodium(I) and iridium(I) complexes.[105]

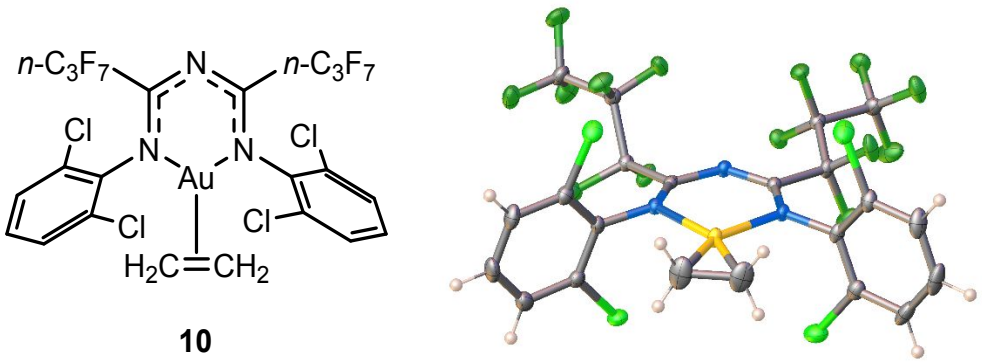

10

Figure 8. [1,5-(2,6-$(Cl)_2$-$C_6H_3)_2$-2,4-(*n*-$C_3F_7)_2$TAP]Au(C_2H_4) (RIZYIJ, **10**) and a view of the crystal structure (**10**).

Shortly after the first review article on coinage metal-ethylene complexes containing three gold(I)-ethylene entries,[71] Flores and Dias reported an isolable gold-ethylene complex

utilizing a backbone-fluorinated 1,3,5-triazapentadienyl (TAP) ligand with flanking aryl groups (**10**, Figure 8, 55% yield), as well as the related copper(I)-ethylene complex (RIZYOP).[44] These complexes feature the TAP ligand in a κ^2 "U-shaped" coordination mode, as opposed to the κ^1 "W-shaped" coordination mode observed with the silver(I)-isocyanide complex.[106] Compound **10** does not lose ethylene under reduced pressure and is air and light stable for more than 1 month at room temperature as a solid. In a solution of chloroform-*d* the NMR shows no decomposition, even after a week of storage. It does not undergo exchange with excess ethylene based on ^{1}H NMR experiments. Both complexes were employed as carbene transfer catalysts using ethyl diazoacetate and cyclopentane, styrene, and benzene. The gold complex **10** gave the sp^3 C-H insertion product of cyclopentane in 42% yield, the cyclopropanation and aromatic C-H insertion products of styrene in 69% and 2% yield respectively, and the Buchner ring expansion and sp^2 C-H insertion product of benzene in 68% and 8% yield respectively (Scheme 1).

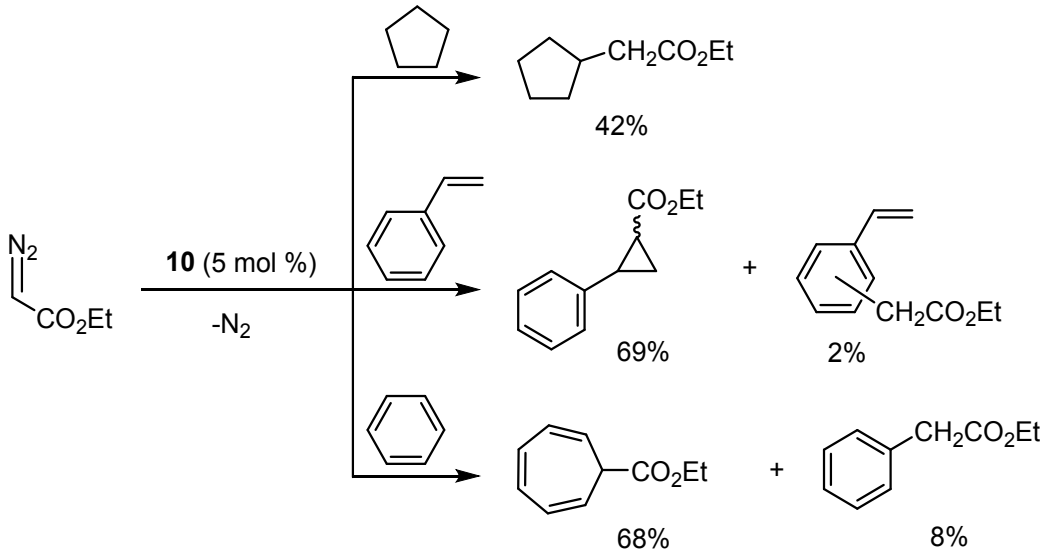

Scheme 1. Carbene addition/insertion reactions of EDA with cyclopentane, styrene, and benzene catalyzed by **10**.

Cationic Gold(I)-Ethylene Complexes

The very first structurally authenticated cationic gold(I)-ethylene complex was reported by Dias *et al.* in 2008.[107] While attempting to prepare a linear gold(I)-ethylene complex "$AuCl(C_2H_4)$", colorless crystals of poor quality were obtained amongst a mixture of black decomposition products. However, preliminary X-ray analysis indicated the serendipitous and unprecedented homoleptic gold(I)-tris ethylene complex with a tetrachloroaurate counter anion ($[Au(C_2H_4)_3][AuCl_4]$). Based off this unexpected result, they set out to intentionally isolate and characterize this complex using a less reactive, commercially available anion, hexafluoroantimonate. By performing the salt metathesis of AuCl with $AgSbF_6$ under an ethylene atmosphere in dichloromethane, the Dias group was able to successfully isolate the desired compound, $[Au(C_2H_4)_3][SbF_6]$ (**11**, Figure 9) as a colorless and crystalline product. This compound is extremely air sensitive, but with special care was characterized by ^1H, $^{13}C\{^1H\}$ NMR, Raman spectroscopy, and X-ray crystallography. Interestingly, all three ethylene moieties are coplanar, arranged in a "spoke-wheel" manner. The isoelectronic nickel(0) species ($[Ni(C_2H_4)_3]$) first reported by Günther Wilke in 1973[108] was also suspected to have this spoke-wheel arrangement of ethylene moieties, possibly leading to homoconjugation and homoaromaticity.[109, 110] In this same report, the copper(I) and silver(I) species were also prepared, but were not able to be completely characterized by X-ray crystallography until 2013.[111]

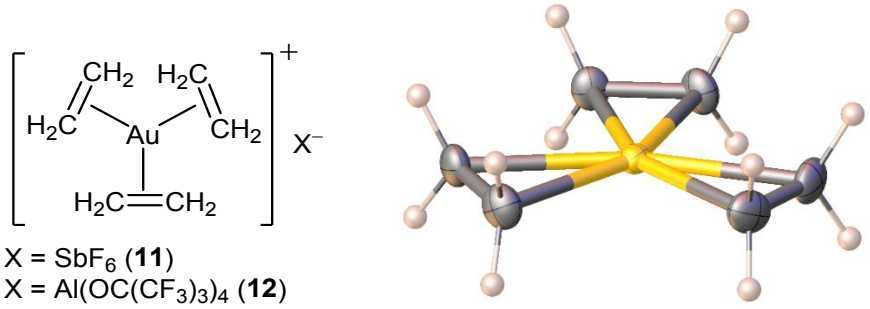

Figure 9. $[Au(C_2H_4)_3][X]$, $[X]^- = [SbF_6]^-$ (KISVOY, **11**), $[Al(OC(CF_3)_3)_4]^-$ (ZETNUJ, **12**) and a view of the crystal structure (**11**, anion omitted).

Later, in 2013, Krossing and co-workers would complete their isostructural series by preparing a similar gold(I)-tris(ethylene) complex with a weakly coordinating tetrakis(nonafluoro-*t*-butoxy)aluminate anion ($[Au(C_2H_4)_3][Al(OC(CF_3)_3)_4]$), **12**.[112] Using the same anion, Santiso-Quiñones *et al.* had previously reported the copper(I)-tris(ethylene) complex in 2007,[113] and the silver(I) complex in 2009 by Reisinger *et al*.[114] These M(I)-tris(ethylene) complexes or modified versions utilizing different counter anions would later be utilized by many groups to isolate cationic ethylene complexes.

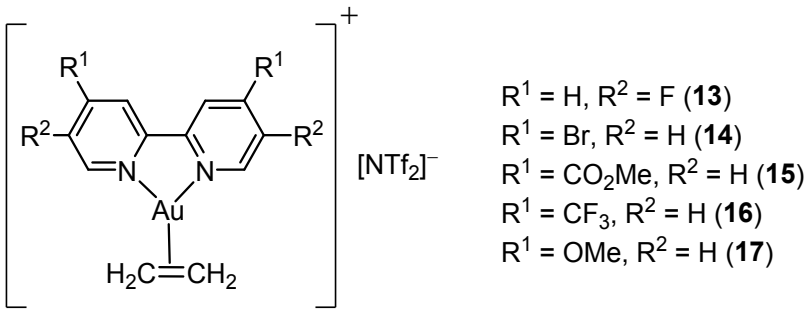

Figure 10. Structurally authenticated $Au(C_2H_4)$ complexes supported by 4,4'-$(R^1)_2$-5,5'-$(R^2)_2$-2,2'-bipyridine.

There was some early work on cationic gold(I) olefin complexes featuring 6-substituted-2,2'-bipyridine supporting ligands by Cinellu and co-workers in 2006,[43] but the results were

limited to NMR spectroscopic data with the exception of the styrene complex which was characterized with single crystal X-ray crystallography. Later, in 2018,[115] the Russell group out of Bristol prepared the cationic 5,5'-difluoro-2,2'-bipyridine gold(I)-ethylene bis(triflyl)amide complex in a 62% yield (**13**, Figure 10), and employed the ethylene complex as a catalyst for the Au-mediated Negishi-type coupling of aryl iodides with different organometallic nucleophiles (Scheme 3). The gold(I)-ethylene complex was prepared by the addition of the 5,5'-difluoro-2,2'-bipyridine ligand to the *in situ* generated gold(I)-tris(ethylene) bis(triflyl)amide in a manner similar to Dias using $AgNTf_2$ in place of $AgSbF_6$. It features a κ^2-coordinated bipyridine ligand with a relatively narrow ∠NAuN bite angle (74.57(9)°).

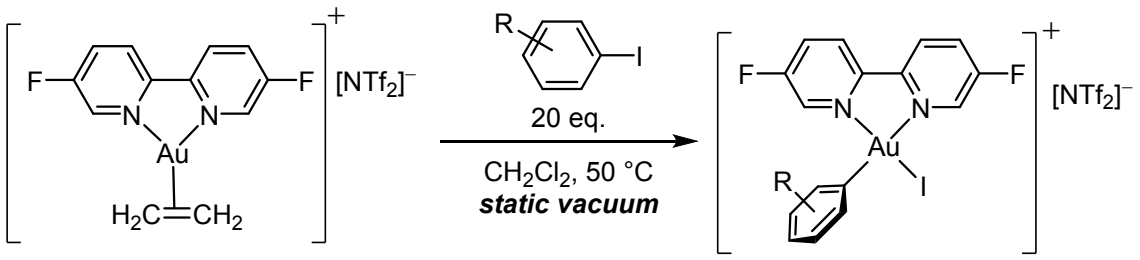

Scheme 2. Oxidative addition of iodoarenes onto **13**.

The Au(I)-ethylene complex undergoes oxidative addition with various aryl iodides (20 equivalents) under static vacuum with moderate heating (50 °C) in good yields (Scheme 2, 57–84%), furnishing square-planar Au(III) d^8 complexes (isoelectronic with Pd(II)) which were also characterized with single crystal XRD, ESI-MS, and NMR spectroscopy. Both electron-rich aryl iodides (*e.g.,* 1-iodo-2-methoxybenzene (72%), 2-iodo-1,3-dimethoxybenzene (78%)) and electron-poor aryl iodides (*e.g.,* 1-fluoro-4-iodobenzene (84%), 1-iodo-4-(trifluoromethyl)benzene (82%)) were tolerated, as well as 2-iodothiophene (79%). Based on ^{19}F

NMR experiments with 1-fluoro-4-iodobenzene, the oxidative addition product was in equilibrium with the reductive elimination of the ethylene complex. To confirm this, a static vacuum was applied to the sealed tube, and full conversion was observed to the oxidative addition product. After pressurizing with ethylene, they observed nearly quantitative (95%) reductive elimination back to the ethylene complex. The Au(III) complexes were also tested with various organometallic nucleophiles (*e.g., p*-tolyl[M], [M] = $B(OH)_2$, Bpin, $SiMe_3$, MgBr, Li, Sn(*n*-Bu)$_3$, ZnCl, *etc.*), with the greatest cross-coupling from *p*-tolylzinc chloride (Scheme 3).

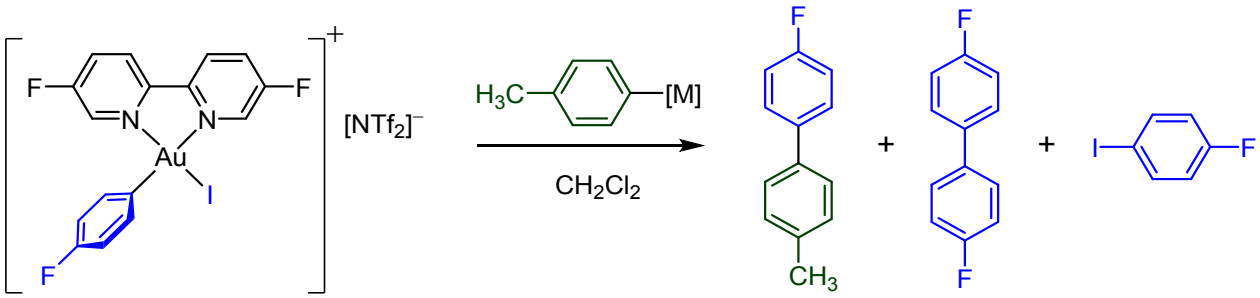

Scheme 3. Cross-coupling of Au^{III} intermediate with organometallic nucleophiles.

Later, in 2021, Russell and co-workers would further investigate this reaction by modifying the substituents on the 4,4' and 5,5' positions (electronic effects), 6,6' positions (steric effects), as well as the counter anion.[116] In this work, they prepared 13 cationic gold(I)-ethylene complexes in yields ranging from 14–38%, and structurally characterized 4 of them with single crystal XRD (**14**–**17**, Figure 10). Both the ^{13}C chemical shift (δ) of the olefinic carbons as well as the Raman shift ($\nu_{C=C}$) were correlated with the Hammett electronic parameters (σ), both yielding a linear relationship. Electron-donating substituents (*e.g.,* R^1 = OMe, *t*-Bu) had the greatest Au->π^*_{C2H4} back-donation based on the large chemical shifts and Raman shift, and electron-withdrawing groups (*e.g.,* R^1 = NO_2, CN, CF_3, CO_2Me) had the lowest extent of back-donation.

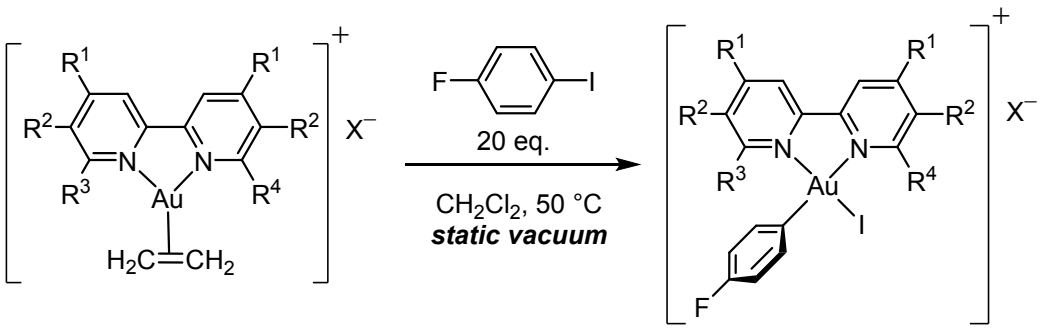

Scheme 4. Oxidative addition of *p*-fluoroiodobenzene with various 2,2'-bipyridine supported Au^{I} complexes.

The influence of ligand electronics on the rates of oxidative addition into aryl-iodides was also investigated, by comparing the initial rates ($\log(k_R/k_H)$) *vs*. σ when the cationic gold(I)-ethylene complexes were reacted with 20 eq. of *p*-fluoroiodobenzene, which revealed a reaction rate constant (ρ) of 0.83 ($R^2 = 0.99$) determined by ^{19}F NMR, where the complexes with electron-withdrawing substituents (*e.g.,* $R^1 = CF_3$) reacted the fastest, and electron-donating (*e.g.,* $R^1 = {}^{t}Bu$) the slowest, with R^1 = OMe reacting too sluggishly to obtain meaningful data (Scheme 4). This trend is opposite to that of kinetic studies of different *p*-substituted triarylphosphine-ligated Pd^0 complexes undergoing oxidative addition (Pd^0/Pd^{II} being analogous to Au^{I}/Au^{III}), wherein the complexes bearing electron-donating substituents reacted the fastest (ρ = -2.8).[117] Although they were able to prepare the gold(I)-ethylene complex using the sterically demanding 6,6'-dimethyl-2,2'-bipyridine ligand in a 26% yield, this complex did not undergo oxidative addition with *p*-fluoroiodobenzene, likely due to steric clash in the square planar geometry of the oxidative addition product. However, the monosubstituted gold(I) complex supported by 6-methyl-2,2'-bipyridine (isolated in 30% yield) did undergo oxidative addition at less than 10% conversion based on ^1H NMR, even at elevated temperatures of 90 °C. The effect of the anion was also

investigated by preparing 5,5'-difluoro-2,2'-bipyridine gold(I) complexes using various anions ($[SbF_6]^-$ (41% yield), $[BF_4]^-$ (19% yield), $[NTf_2]^-$ (60% yield)), however the difference in the observed rate was negligible, largely unaffected by the counter anion. Despite this, it is likely that the use of a more strongly coordinating anion such as triflate could suppress π-coordination of olefins or the oxidative addition of aryl iodides, reducing the rate as observed by Amgoune and Bourissou and co-workers.[66]

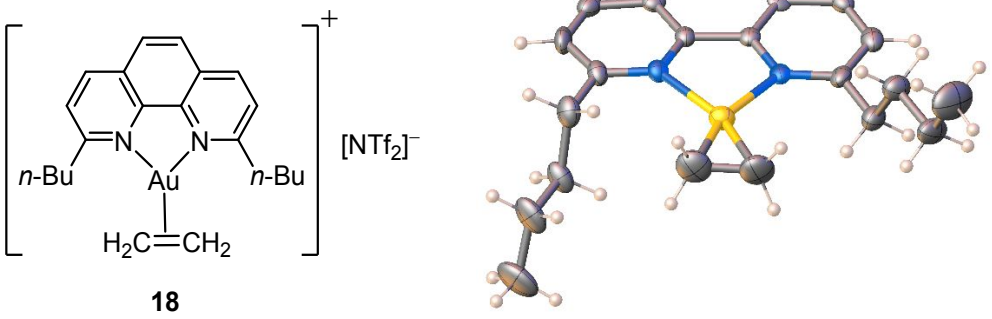

18

Figure 11. [2,9-(*n*-Bu)$_2$PhenAu(C_2H_4)][NTf_2] (ROFQOV, **18**) and a view of the crystal structure (anion omitted).

In 2019, Hashmi and co-workers reported a gold-catalyzed direct alkynylation of cyclopropenes utilizing a mixed Au/Ag co-catalysis system, achieving the first cyclopropene alkynylation by C-H activation.[118] They began their investigation by first optimizing conditions for the reaction (Scheme 5), using the ester functionalized cyclopropene and the hypervalent ethynylbenziodoxole with the best conditions shown.

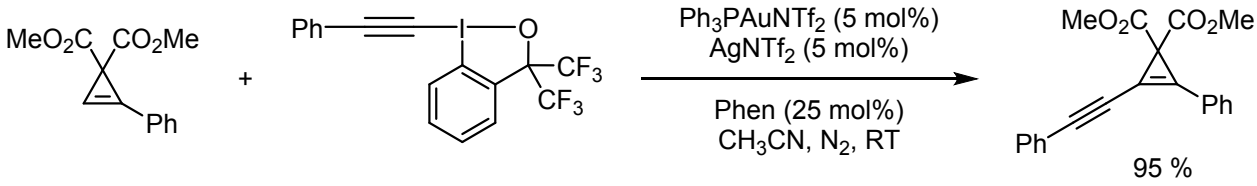

Scheme 5. Optimized conditions for cyclopropene C_{sp2}-H alkynylation catalyzed by Au^{I}/Ag^{I}.

Based off the preliminary work of Russell which used a substituted 5,5'-difluoro-2,2'-bipyridine ligand supported Au^{I}(ethylene) complex **13** which underwent oxidative addition with aryl iodides, Hashmi and co-workers proceeded through a similar route using a hypervalent alkynyl iodane. They first prepared the $[(Phen)Au(C_2H_4)][NTf_2]$ species (**18a**) in 15% yield and used this as a pre-catalyst in place of $Ph_3PAuNTf_2$ and phenanthroline, resulting in a 95% NMR yield in 5 minutes. Additionally, a gold(I)-ethylene complex using 2,9-di-*n*-butyl-1,10-phen was prepared (**18**, Figure 11) in a 17% yield, however this did not yield any cyclopropene alkynylation, likely due to steric clash of the *n*-butyl groups hindering oxidative addition. The aforementioned 5,5'-difluoro-2,2'-bipyridine supported complex reported by Russell (**13**) gave a 72% yield for the cyclopropane alkynylation.

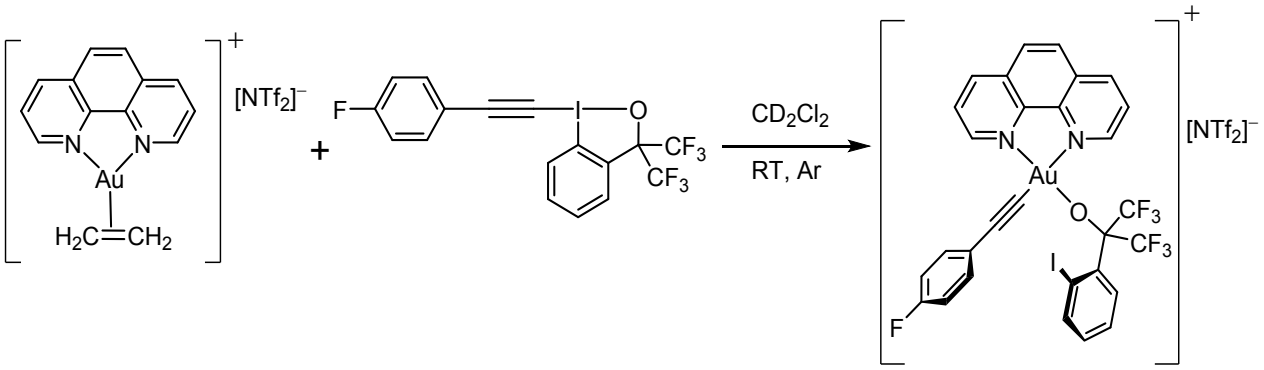

Scheme 6. Oxidative addition of $[(Phen)Au(C_2H_4)][NTf_2]$ (**18a**) with (4-fluorophenyl)ethynylbenziodoxole.

The ethylene complex **18a** was treated with (4-fluorophenyl)ethynylbenziodoxole, which quantitatively furnished the oxidative addition product, characterized by 1D and 2D NMR.[118] Upon crystallization, they obtained a mixed Au^{I}/Au^{III} structure, where one additional $(Phen)Au^{+}$ fragment is chelated to the Au^{III} acetylide in a π-fashion. The $(Phen)Au^{+}$ species likely arose during crystallization due to alkynyl scrambling and reductive elimination to the diyne and Au^{I}.

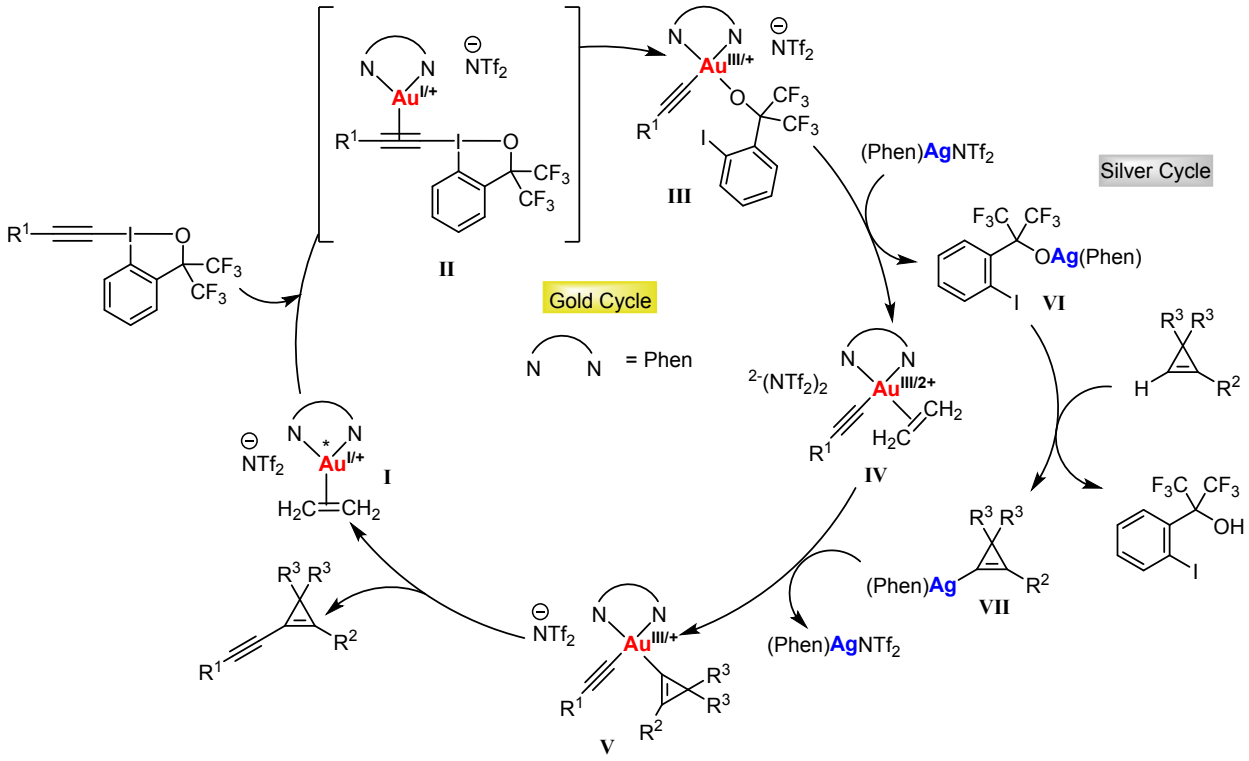

Scheme 7. Proposed mechanism of cyclopropene alkynylation, featuring two co-operative cycles. *The superscripts represent the oxidation state and the net charge, *e.g.,* $Au^{III/+}$ represents gold(III) with two anionic ligands, net charge of +1.

Based on their experiments and previous literature,[119-121] the above mechanism (Scheme 7) was proposed, comprised of two separate gold and silver cycles. The silver cycle is supported

by independent experiments of H/D exchange of cyclopropene with D_2O, $AgNTf_2$, phenanthroline, as well as α,α-bis(trifluoromethyl)benzyl alcohol and cesium carbonate to generate a comparable silver(I) alkoxide unit *in situ*, achieving 76% cyclopropene deuteration within 10 minutes. Recent work from Larrosa,[119] Sanford,[120] and Hartwig[122] has revealed that silver(I) salts can cleave acidic C-H bonds of certain arenes and heteroarenes. Cyclopropene C-H bonds are relatively acidic ($pK_a \approx 30$), due to similar hybridization to alkynes.[121] The gold cycle begins with ethylene displacement of **I** by the ethynylbenziodoxole, followed by oxidative addition to the $Au^{III/+}$ species **III**. The alkoxide anion then undergoes metathesis with $(Phen)AgNTf_2$, yielding the highly electrophilic $Au^{III/2+}$ species **IV** and the silver(I) alkoxide **VI**. The crucial importance of ethylene as a stabilizing placeholder ligand is apparent in stabilizing **IV**, as in the absence of ethylene, **III** undergoes immediate decomposition upon addition of $AgNTf_2$, giving no yield of the desired cyclopropene. The silver(I) cyclopropenyl intermediate **VII** from the silver cycle then undergoes transmetallation with **IV** yielding **V**, which can undergo reductive elimination returning to **I** and furnishing the alkynylated cyclopropene. The transformation was studied with various R^1 (aryl, heteroaryl, alkyl, TIPS (Si(*i*-Pr)$_3$)) giving isolated yields of 61–89%, R^2 (aryl, alkyl, cycloalkyl) giving isolated yields of 44–92%. In all cases, R^3 was CO_2Me, except for one instance of CO_2Et ($R^1 = R^2 = Ph$) with a yield of 61%.

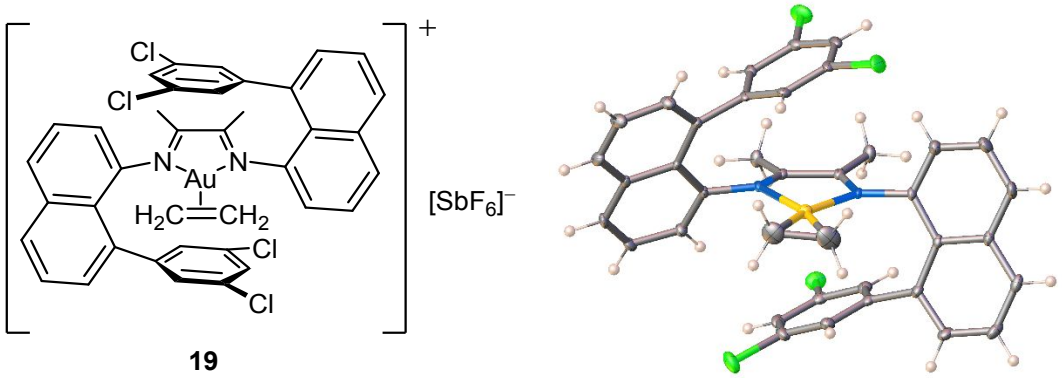

19

Figure 12. [(*N,N'*-(8-(3,5-(Cl)$_2$-C$_6$H$_3$)-1-Nt)butane-2,3-diimine)Au(C$_2$H$_4$)][SbF$_6$] (OWEYOG, **19**) and a view of the crystal structure (anion has been omitted for clarity).

A rare isostructural series of cationic coinage metal (copper, silver, gold) ethylene complexes supported by nitrogen ligands were reported in 2016 by Daugulis and co-workers, utilizing a diimine ligand with flanking 8-aryl-1-naphthyl groups creating a "sandwich-type" complex (**19**, Figure 12).[123] The ligand itself was prepared using a C-H functionalization they had published in 2013,[124] by coupling 3,5-dichloro-1-iodobenzene with picolinic acid 1-napthylamide using Pd(OAc)$_2$ (5 mol%) with silver(I) acetate as a base and halide sequestering agent to selectively yield the C8 arylation in a 77% yield in the absence of solvent. The amide was then hydrolyzed with base to the amine, and finally condensed with butane-2,3-dione to give the ligand in 86% yield. The copper(I) complex has been prepared from copper(I) triflate under an ethylene atmosphere, or by addition of the ligand to [Cu(C$_2$H$_4$)$_3$][SbF$_6$] (generated from CuI and AgSbF$_6$ following the method reported by Dias).[111] The silver(I) and gold(I) complexes were also prepared in a similar manner with [SbF$_6$]$^-$ as the counter anion, with a 42% yield for the gold(I) complex **19**. All three crystal structures revealed the expected κ^2 coordination from the diimine, with the 3,5-dichlorophenyl groups sandwiching the metal center. The gold(I) complex **19**

decomposes in solution within one hour at room temperature, but as a solid it can be stored in a -20 °C freezer for several months. Interestingly, this gold(I) ethylene complex displayed an AA'BB' spin system in the ^{1}H NMR, similar to the κ^2-hydrotris(3,5-di(*t*-butyl)-pyrazolyl)borate gold(I) ethylene complex (**5**). This can possibly be rationalized by a strong gold-ethylene bond which minimizes association/dissociation, and hindered rotation of ethylene due to the flanking aryl rings. Ethylene exchange studies were performed for all three complexes by means of variable temperature ^{1}H NMR and Erying analysis based on the temperature at which the signals for bound and free ethylene coalesced. The analysis revealed that the silver complex exchanges the fastest, and gold the slowest, with copper being an intermediate. Additionally, the gold(I) ethylene complex was purged at -30 °C with labeled ethylene-d_4, giving a 97% conversion to the deuterium labelled complex, followed by addition of an excess of unlabeled ethylene, and the rate of ethylene exchanged was monitored from 199 to 214 K. Erying analysis of C_2D_4/C_2H_4 exchange from 199 to 214 K yielded a negative value for the activation entropy ($\Delta S^{\ddagger}$ = -22.5 ± 4.8 cal K^{-1} mol^{-1}), which is consistent with an associative ligand substitution mechanism.

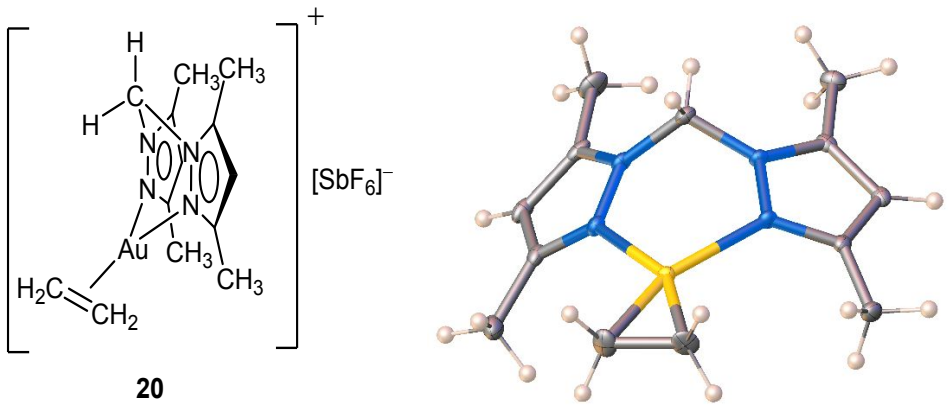

20

Figure 13. $[H_2C(3,5\text{-}(CH_3)_2\text{-}Pz)_2)Au(C_2H_4)][SbF_6]$ (HAYYEP, **20**) and a view of the crystal structure (anion has been omitted for clarity).

In 2022 the Dias and Roithová groups collaborated and investigated a systematic series of bis(pyrazolyl)methane supported coinage metal complexes of various alkenes and alkynes to further probe what affects the metal-(π-ligand) interaction by varying the supporting ligand, metal center, and bound π-ligand .[86] In this report, they described an isostructural series of copper(I), silver(I), and gold(I)-ethylene complexes supported by the bis(3,5-dimethyl-1-pyrazolyl)methane ligand (**20**, Figure 13), as well as the copper(I) and silver(I) ethylene complexes supported by the electron-withdrawing bis(3,5-bis(trifluoromethyl)-1-pyrazolyl)methane ligand. The gold(I) complex (20) was prepared in a 78% yield by the addition of a solution of the ligand to *in situ* generated $[Au(C_2H_4)_3][SbF_6]$ (**11**). Copper(I) complexes of 1-pentene, 1- and 2-pentyne were also reported. The NMR and XRD data were corroborated with mass spectroscopic studies by the Roithová group, including Helium tagged IR photodissociation spectra of 1-pentyne complexes in the gas phase and collision induced dissociation (CID) experiments to determine the experimental bond dissociation energy (BDE). The results from the mass spectroscopic studies agreed well with the experimental NMR data and previous reports on isostructural series.

The trend amongst metals is that the greatest interaction is between gold and the π-ligand (BDE_{exp} 1.75–2.11 eV, 40.4–48.7 kcal mol^{-1}), and the weakest is between silver and the π-ligand (BDE_{exp} 1.20–1.41 eV, 27.7–32.5 kcal mol^{-1}), with copper being intermediate (BDE_{exp} 1.46–1.73 eV, 33.7–39.9 kcal mol^{-1}). The electron density at the metal was varied by changing the donating/withdrawing nature of the supporting ligand, and the result was that for silver complexes the binding energies slightly increase by changing from a donating to withdrawing ligand (*e.g.,* 1.21 eV/27.9 kcal mol^{-1} for the electron-donating ligand to 1.31 eV/30.2 kcal mol^{-1} for the electron-withdrawing ligand), slightly decrease for gold, and stay about the same for copper. This would suggest that π-back bonding grows following Ag<Cu<Au and is the dominating orbital interaction for gold π-complexes, which is in good agreement with other reports.[84, 94, 123]

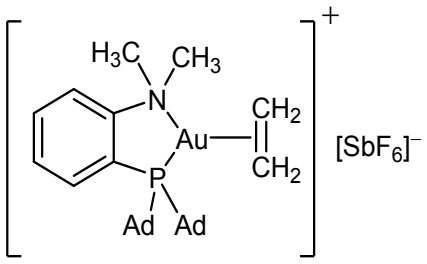

21

Ad = 1-Adamantyl

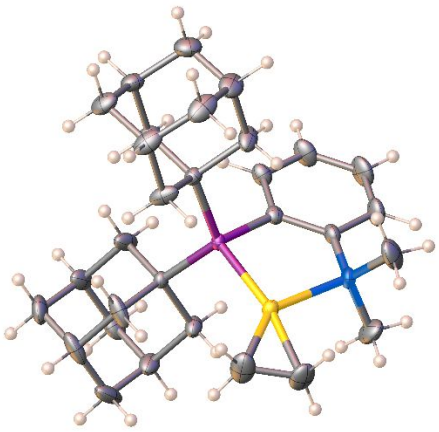

Figure 14. [(MeDalphos)Au(C_2H_4)][SbF_6] (GUCBAK, **21**) and a view of the crystal structure (anion omitted).

In 2019, Bourissou and Amgoune reported on a Au^{I}/Au^{III} catalyzed arylation and heteroarylation of 1-R-indoles (R = H, CH_3) with high regioselectivity for C3 (hetero)arylation, using a cationic gold(I) complex supported by the hemilabile (P,N) MeDalphos ligand (1-(NMe_2)-

2-P(1-Ad)$_2$-C$_6$H$_4$) with various aryl iodides as well as 2-iodo-pyridine and 3-iodo-thiophene.[125] The following year, based on this preliminary work as well as aforementioned work done by Russell[115, 116] and Hashmi,[118] Bourissou sought to investigate the versatility and behavior of the MeDalphos ligand, by preparing a series of cationic gold(I) π-complexes using electron-rich, electron-deficient, and unbiased alkenes.[126] They prepared the (MeDalphos)AuCl complex, followed by salt metathesis with $AgSbF_6$ in the presence of an electron-rich alkene (3,4-dihydro-2*H*-pyran, DHP, 77% yield), electron-unbiased alkenes/alkynes (ethylene (**21**, Figure 14, 89% yield), 1-hexene (63% yield), styrene, 3-hexyne (50% yield)), and the first electron-deficient alkene gold complexes in literature (methyl acrylate (68% yield), *N*-phenylmaleimide), all as air stable solids, with the exception of the *N*-phenylmaleimide complex (Scheme 8).

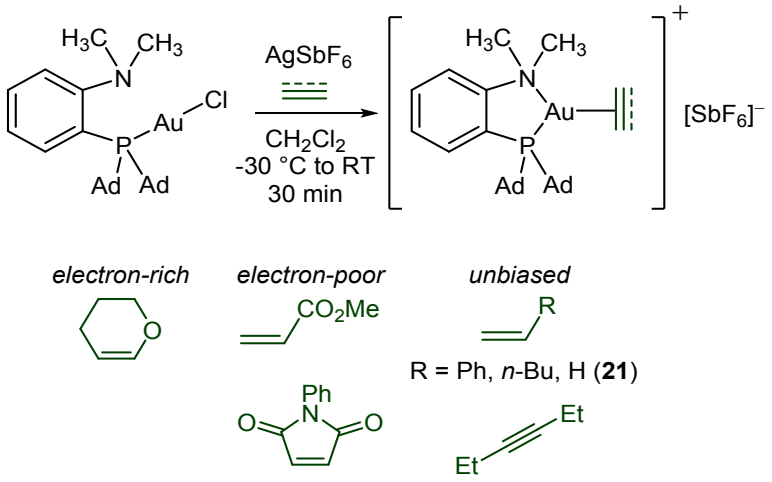

Scheme 8. Synthesis of [(MeDalphos)Au(π-ligand)][SbF_6] with various alkenes/alkynes.

The olefinic protons and carbons of the bound alkenes all showed the typical upfield shifts (1.0–2.1 ppm in ^{1}H, 37.0–65.3 ppm in ^{13}C) with the exception of the electron-rich DHP complex which featured an unusual downfield shift of 1.42 ppm in the ^{1}H NMR. Interestingly, the ^{1}H and

^{13}C resonances for the dimethylamino groups, as well as the ^{31}P resonance of the di(1-adamantyl)phosphino group correlated to the electronic properties of the bound π-ligand. When compared to the (MeDalphos)AuCl complex, the electron-deficient complexes featured downfield shifts (Δδ) of the $N(CH_3)_2$ groups ranging from 0.5–0.87 ppm in the ^{1}H NMR and downfield shifts ranging from 6.8–8.4 ppm in the ^{13}C NMR, as well as downfield shifts of 9.6 and 11.7 ppm in the ^{31}P NMR. In contrast, the electron-rich DHP complex had slighter downfield shifts of 0.14, 0.17 ppm in the ^{1}H NMR, 2.3, 2.5 ppm in the ^{13}C NMR, and 2.9 ppm in the ^{31}P NMR. The electron-unbiased complexes had intermediate values in all NMR spectra. This supports the hemilability of the supporting MeDalphos ligand, as based on NMR data the ligand adjusts its coordination to gold(I) in response to the electronics of the bound π-ligand. This is further corroborated by comparing the Au-P and Au-N bond distances of selected complexes. The Au-P distance in the electron-rich DHP complex was reported to be 2.3032(6) Å, which elongates to 2.334(2) Å in the electron-deficient *N*-phenylmaleimide (NPM) complex. In contrast, the Au-N bond distance for the DHP complex (2.505(2) Å) contracts to 2.234(6) Å for the NPM complex. Computational studies further supported the hemilabile nature of the MeDalphos ligand. The most noteworthy correlation was between the Au-N bond strength with the Au-(π-ligand). As the π-ligand becomes more electron-deficient, the dimethylamino group accommodates this by increasing its donation to gold, based on NMR, bond distance, and computational data.

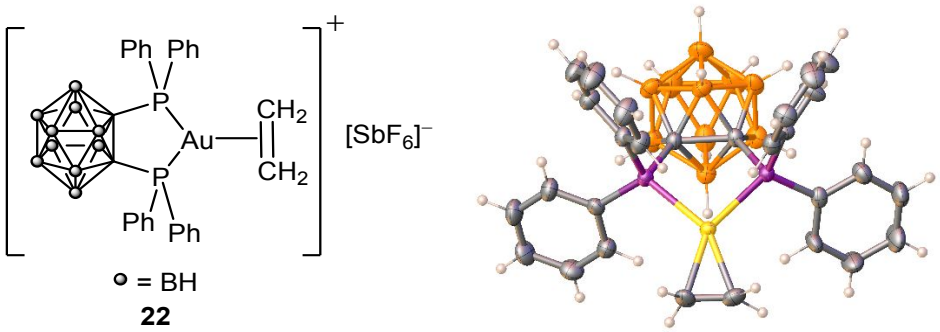

Figure 15. [(*o*-$(PPh_2)_2$-dicarborane)Au(C_2H_4)][SbF_6] (GUCBUE, **22**) and a view of the crystal structure (anion omitted).

In order to further investigate the role of the hemilability of the MeDalphos ligand, Bourissou next turned to a *P,P* chelating *o*-carboranyl diphosphine ligand which is less flexible in its donor properties compared to the *N,P* chelating MeDalphos. Both the styrene and ethylene (**22**, Figure 15, 84% yield) complexes were characterized, featuring electron-unbiased olefins. However, attempted syntheses with electron-rich and electron-deficient π-ligands were unsuccessful. Both electron-deficient alkenes (methylacrylate and NPM) were observed and unambiguously characterized by ^{1}H and ^{31}P NMR in the presence of excess ligand but attempts at isolation were unsuccessful due to decomposition. The inability of the *P,P* supporting ligand to stabilize electronically biased alkenes further supports the utility of using a hemilabile ligand such as MeDalphos. To probe catalytic relevance, they investigated the hydroarylation of alkenes using 1-methylindole, catalyzed by (MeDalphos)AuCl/$KB(C_6F_5)_4$ (5 mol%) in chloroform at 135 °C. The electron-deficient alkenes (methylacrylate and NPM) gave 75% and 40% conversion respectively (NMR yields) after 24 hours, and the electron-rich DHP resulted in the quantitative double indole addition after ring opening of the tetrahydropyran intermediate. All reactions gave complete selectivity for the C3-position of indole.

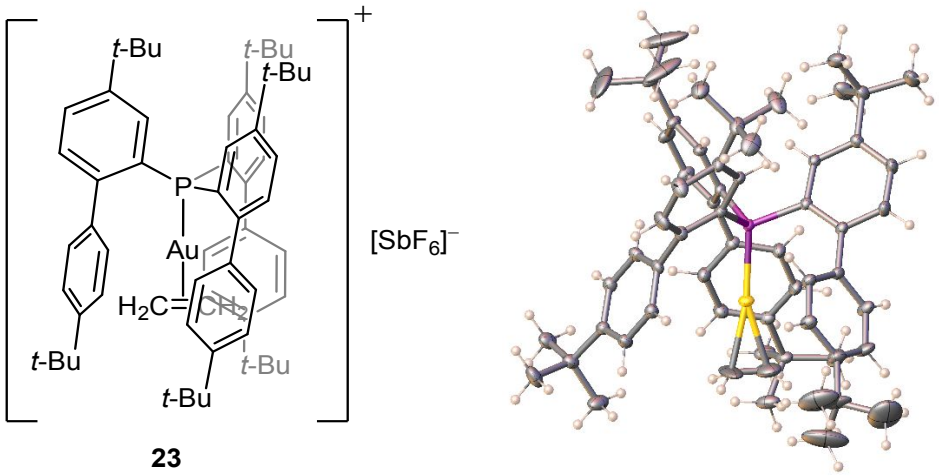

23

Figure 16. [((2-(4-*t*-BuC_6H_4)-5-*t*-Bu-1-C_6H_3)$_3$P)Au(C_2H_4)][SbF_6] (ACADOB, **23**) and a view of the crystal structure (anion omitted).

The first di-coordinate, linear gold(I) ethylene complex was reported in 2021[127] by the Campos group in Sevilla utilizing an extremely bulky tris-(4,4'-di-*tert*-butyl-2-biphenyl)phosphine ligand first reported by Straub.[128] Prior to this publication, there have been reports of di-coordinate gold(I) complexes of substituted alkenes stabilized by sterically demanding NHCs[129, 130] and phosphines[131-134], but all previous efforts to isolate and structurally authenticate a linear gold(I)-ethylene complex were unsuccessful. Campos had previously utilized bulky, terphenyl substituted phosphines to isolate exotic heterobimetallic Au(I)/Pt(0) species and activate dihydrogen and acetylene.[135-137] Initially, the neutral phosphine gold(I) chloride complex was isolated by treatment of Au(THT)Cl (THT = tetrahydrothiophene) with the phosphine to form the air-stable complex in 96% yield. Single-crystal X-ray diffraction revealed that all three *ortho*-aryl groups were oriented around gold, rather than rotated away, ensuring the greatest steric protection with a percent buried volume (%V_{bur}) of 67.0%. Treatment of the gold(I) chloride

complex with $AgSbF_6$ in the absence of ethylene yielded a trimetallic complex featuring two $AgSbF_6$ moieties in the phosphine pocket, highlighting the flexibility of the biphenyl rings to accommodate multiple species in the cavity. In the presence of ethylene, treatment of the gold(I) chloride complex with $AgSbF_6$ successfully yielded the desired ethylene complex in an 83% yield. Crystallization obtained by vapor diffusion of *n*-pentane into concentrated dichloromethane gave two types of crystals. Both feature the linear gold(I)-ethylene complex (*i.e.,* **23**, Figure 16), however the second set of crystals are dimeric, bridged by a $[Ag(C_2H_4)(\mu\text{-}H_2O)]_2$ moiety, likely from unreacted $AgSbF_6$ that was not removed by celite filtration (ACACOA, Figure 17).

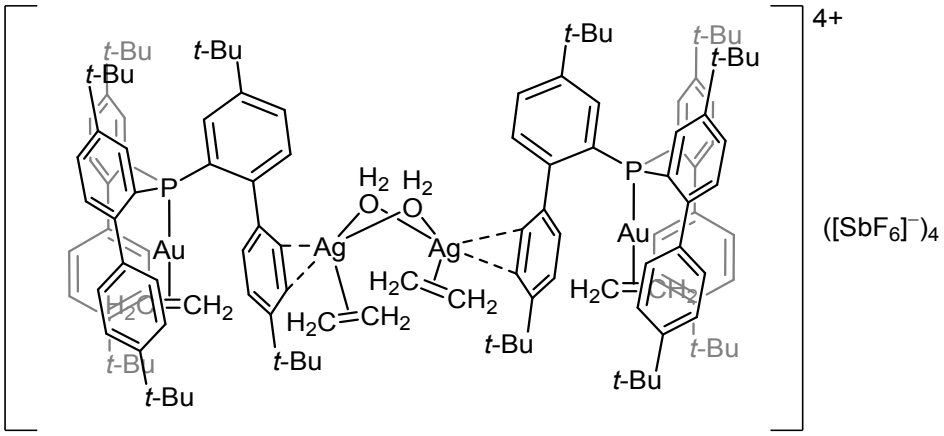

Figure 17. Silver bridged dimeric **23** (ACACOA).

Similar to the gold(I)-ethylene complexes supported by κ^2-hydrotris(3,5-di(*t*-butyl)-pyrazolyl)borate (**5**) from Dias and the di-naphthyl-diimine complex from Daugulis (**19**), this complex featured a distinctive AA'BB' pattern in its ^1H NMR spectrum at 3.79 and 3.66 ppm. This large upfield shift from free ethylene for a monodentate ligand can be rationalized by the proximity of the three phenyl rings and their aromatic ring current effect, as the $^{13}C\{^1H\}$ resonance had a minimal shift of 13.0 ppm from free ethylene, suggested minimal π-

backdonation when compared to other bidentate ligand systems. Similar to Daugulis, Campos performed an Erying analysis from -20 °C to 30 °C using 2D exchange spectroscopy (EXSY) to observe chemical exchange between free and bound ethylene. Based off the Erying plot, the enthalpy ($\Delta H^{\ddagger}$) and entropy ($\Delta S^{\ddagger}$) for the ethylene exchange are 6.7 kcal mol^{-1} and -38.1 cal K^{-1} mol^{-1} respectively, giving a Gibbs free energy ($\Delta G^{\ddagger}_{298}$) of 18.0 kcal mol^{-1} at 298 K. The large negative entropic factor denotes an associative exchange mechanism is at play, involving an intermediate with two ethylene ligands (*i.e.,* [$(R_3P)Au(C_2H_4)_2$][SbF_6]). This is supported by the observance of cross-peaks for free and bound ethylene in the NOESY spectrum, similar parameters reported by Daugulis ($\Delta H^{\ddagger}$ = 10.0 ± 1.4 kcal mol^{-1}, $\Delta S^{\ddagger}$ = -22.5 ± 4.8 cal K^{-1} mol^{-1}, $\Delta G^{\ddagger}_{298}$ = 16.7 ± 0.1 kcal mol^{-1}), as well as the flexibility of the cavity afforded by the tris-(4,4'-di-*tert*-butyl-2-biphenyl)phosphine ligand. The ethylene ligand was able to be displaced by stronger ligands like carbon monoxide and acetonitrile, and NMR exchange experiments unveiled that the gold(I) complex had the greatest affinity for acetonitrile, followed by carbon monoxide, and the lowest affinity for ethylene. Computational analysis of the bonding interaction revealed that π-backdonation plays a minor role in the linear gold(I)-ethylene complex, which contrasts to previously discussed tricoordinate complexes where π-backdonation dominates. This is supported by a slight chemical shift in the $^{13}C\{^1H\}$ NMR, and relatively long Au-C bond lengths (2.216(6) and 2.235(6) Å). The gold bound ethylene C=C bond length was notably shorter compared to that of the free ethylene value of 1.3369(16) Å (determined by electron diffraction methods of gaseous ethylene),[138] perhaps indicating unresolved disorder and/or libration effects of the moiety.

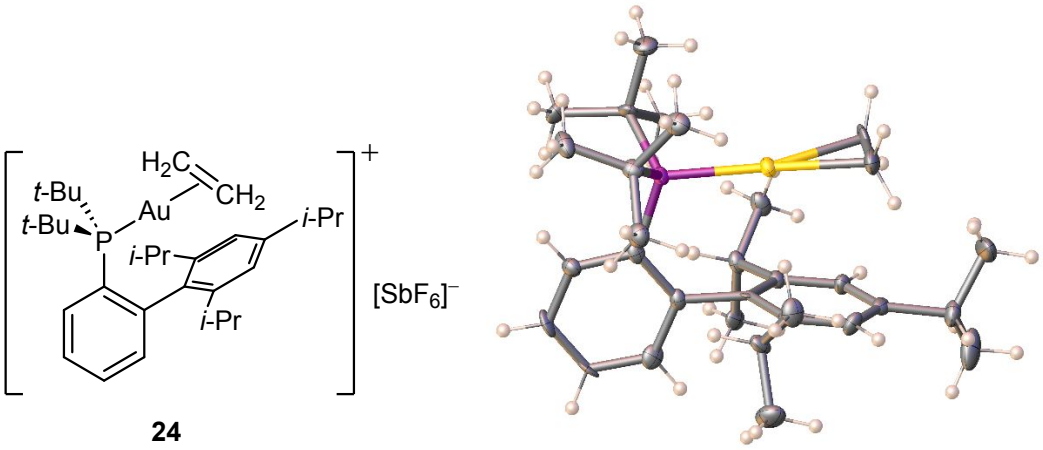

24

Figure 18. [((*t*-Bu)$_2$P(2-(2,4,6-(*i*-Pr)$_3$-C$_6$H$_2$)-C$_6$H$_4$))Au(C$_2$H$_4$)][SbF$_6$] (SILDOK, **24**) and a view of the crystal structure (anion omitted).

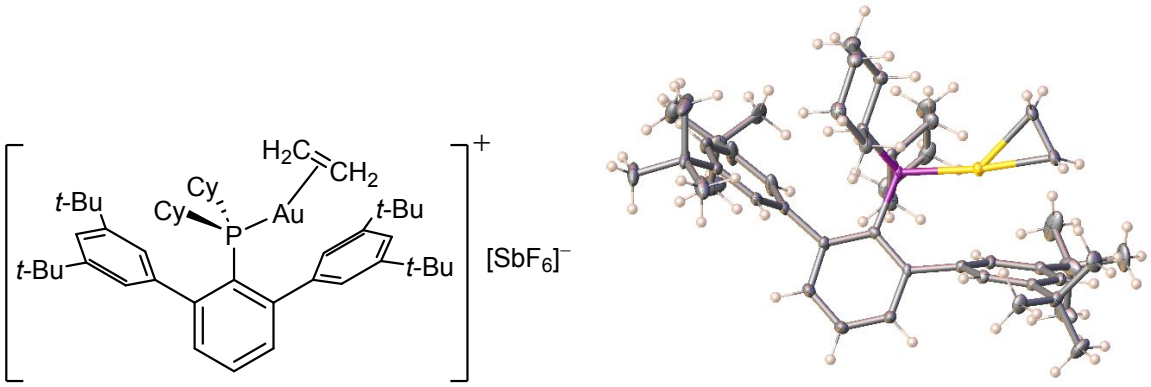

Figure 19. [((Cy)$_2$P(2,6-(3,5-(*t*-Bu)$_2$-C$_6$H$_3$)-C$_6$H$_3$))Au(C$_2$H$_4$)][SbF$_6$] (SILSEP, **25**) and a view of the crystal structure (anion omitted) featuring a slipped ethylene.

Shortly after reporting the first linear gold(I) ethylene complex, the Campos group would go on to prepare seven more in high yields (53–93%), and report the crystal structure of two of them (**24**, Figure 18 and **25**, Figure 19).[139] The gold(I) ethylene complexes were prepared following the previous method, first generating the LAuCl complex by reaction of phosphine ligands (**L1**–**L8**) with Au(THT)Cl, followed by salt metathesis with AgSbF$_6$ under an ethylene

atmosphere. In addition to the previously utilized ligand (**L1**), commercially available trimesitylphosphine (**L2**) and *t*-BuXPhos (**L3**) and terphenyl phosphines (**L4**–**L8**) were used (Figure 20).

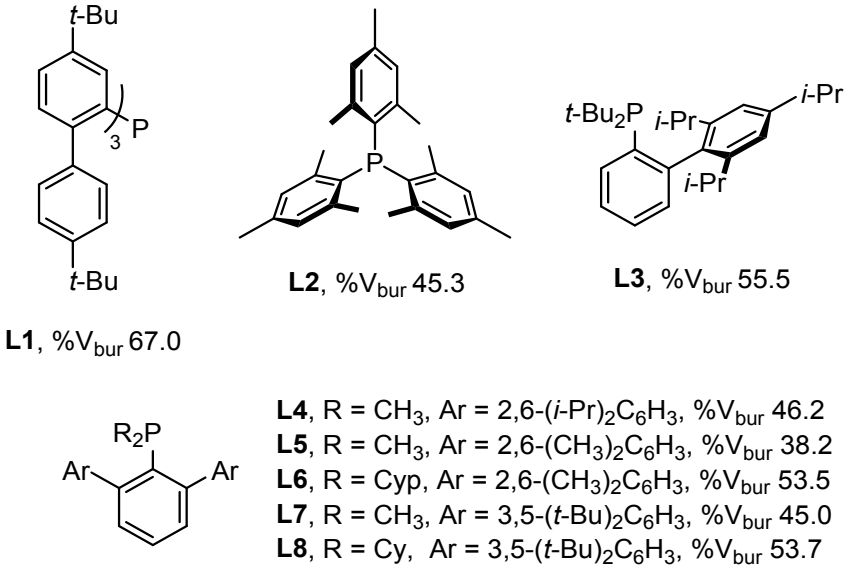

Figure 20. Bulky phosphine ligands used, Cyp = cyclopentyl, Cy = cyclohexyl.

All the complexes displayed an averaged set of resonances for the ethylene protons (singlet, ranging from 4.77 to 5.46 ppm) except for the previously mentioned **L1** complex with its AA'BB' spin system. The $^{13}C\{^{1}H\}$ resonance of the ethylene carbons also displayed slight upfield shifts (Δδ) from free ethylene, ranging from 11.4 to 14.2 ppm, consistent with minimal π-backdonation of the previously reported linear complex. The NMR was recorded in the presence of excess free ethylene to minimize decomposition, evacuation of free ethylene leads to slow decomposition in both solid state and in a dichloromethane solution. This contrasts to the previously reported **L1**Au(C_2H_4) complex which displayed remarkable stability, likely due to the

steric shielding and high $\%V_{bur}$. Crystal structures of the gold(I) ethylene complexes supported by **L3** (**24**, Figure 18) and **L8** (**25**, Figure 19) were obtained, with C=C distances of 1.353(15) and 1.384(10) Å respectively, which is more in line with typical gold(I)-ethylene complexes. Quite interestingly, the ethylene coordination in **25** is asymmetric, with a slipped ethylene group perpendicular to the plane of the adjacent phenyl ring (for comparison, the ethylene group in **24** is parallel to the phenyl ring). The ∠P-Au-C angles of 137.2(2) and 173.54(19)° are quite different in **25**. It is possible that **25** may be considered as pseudo-trigonal planar at gold. Upon closer inspection, the *ipso* carbon of the flanking phenyl group is 2.736 Å from gold, which is within the sum of van der Waals radii. Additionally, the sum of bond angles at gold are 359.68° (∠P-Au-C_{cent} = 155.30°, ∠P-Au-C_{ipso} = 78.35°, ∠C_{ipso}-Au-C_{cent} = 123.03°, where C_{cent} is the centroid between the ethylene carbons and C_{ipso} is the *ipso* carbon of the flanking phenyl group).

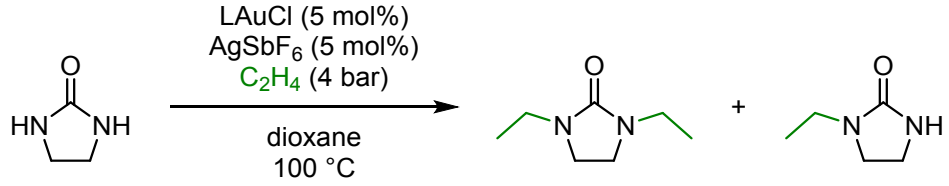

Scheme 9. Ethylene hydroamination of imidazolidine-2-one.

These complexes were then investigated as catalysts for the hydroamination of ethylene using imidazolidine-2-one as a diamine. Complexes supported by bulky phosphine ligands (**L1**, **L3**, **L6**, **L8**, $\%V_{bur}$ 53.5–67.0) reached full conversion of the double hydroaminated 1,3-diethylimidazolin-2-one within 18 hours, with no detection of the mono hydroaminated product. Less sterically demanding ligands (**L2**, **L4**, **L5**, **L7**) with $\%V_{bur}$ ranging from 38.2 to 46.2 gave little to no conversion. To confirm silver(I) had no role in the transformation (other than halide

abstraction), the ethylene complex ([**L1**Au(C_2H_4)][SbF_6], **23**) was also employed, yielding full conversion to the double hydroaminated product. Likewise, in the presence of $AgSbF_6$ and **L1** or **L2** but the absence of gold, no conversion is obtained, revealing silver(I) is not capable of catalyzing this reaction. When the acetonitrile complex ([**L1**Au(NCMe)][SbF_6]) is employed, full conversion is obtained at 2 bar of ethylene, but at lower pressures (*i.e.,* 1 bar) only 50% conversion is obtained, likely due to competitive coordination at gold. Reactions utilizing proton shuttles (*i.e.,* 0.1–10 eq. H_2O or hexafluoro-*iso*-propanol, HFIP) showed no significant effects, however acids like triflic or acetic acid reduced conversion, and bases such as KO*t*Bu, DBU, Et_3N completely ceased the reaction. This evidence, along with $^{31}P\{^1H\}$ NMR and computational studies support the below mechanism.

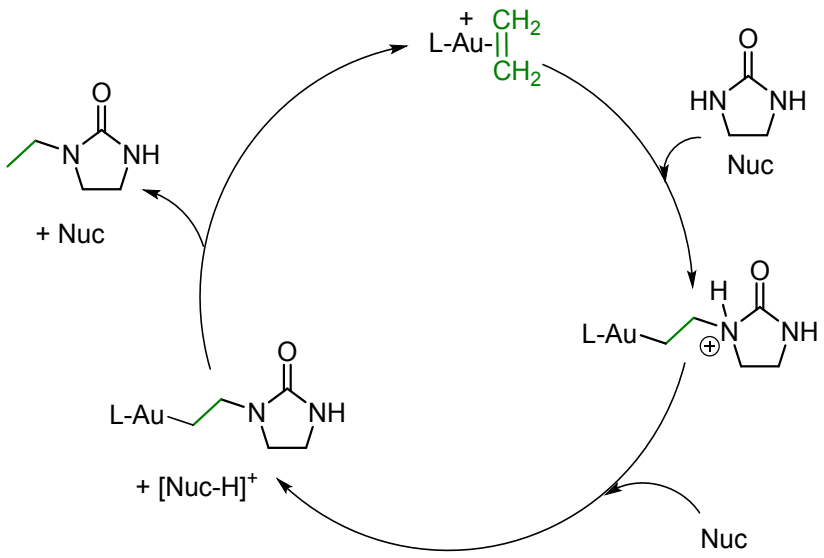

Scheme 10. Proposed hydroamination mechanism, Nuc = imidazolidine-2-one.

Structural and spectroscopic features and trends

Table 1. Structurally authenticated, gold(I) ethylene complexes. (a) $CDCl_3$ (b) CD_2Cl_2 (c) toluene-d_8 (d) -20 °C (e) -60 °C (f) resolved AA'BB' system. The $\Delta\delta^1H$ and $\Delta\delta^{13}C$ values in parentheses represent the change in chemical shift for the protons and carbons of ethylene (*i.e.,* ($\Delta\delta = \delta_{bound} - \delta_{free}$)). *Two or more molecules in the asymmetric unit. [#]Gold-ethylene moiety disorder. [†]Range and average values are given when a given molecule has more than two chemical similar parameters.

CSD Refcode	Compound	Au-C, Å	$H_2C=CH_2$, Å	δ^1H ($\Delta\delta^1H$), ppm	$\delta^{13}C$ ($\Delta\delta^{13}C$), ppm
CIMXAY	κ^2-[HB(3,5-$(CF_3)_2$-Pz)$_3$]Au(C_2H_4) (**1**)	2.096(6), 2.108(6)	1.380(10)	3.81 (-1.59)[a]	63.7 (-59.4)[a]
CIMXEC	κ^2-[HB(3-CF_3-5-Ph-Pz)$_3$]Au(C_2H_4) (**2**)	2.093(5), 2.096(5)	1.387(9)	3.69 (-1.71)[a]	59.3 (-63.8)[a]
IREBEO[#]	κ^2-[HB(3-CF_3-5-CH_3-Pz)$_3$]Au(C_2H_4) (**3**)	2.084(11), 2.088(11)	1.40(2)	3.49 (-1.91)[b]	58.6 (-64.6)[b]
OKOQEN	κ^2-[HB(3,5-$(Ph)_2$-Pz)$_3$]Au(C_2H_4) (**4**)	2.100(5), 2.082(4)	1.413(7)	2.61 (-2.79)[b,d]	55.3 (-67.9)[b,d]
OKOQIR	κ^2-[HB(3,5-(*t*-Bu)$_2$-Pz)$_3$]Au(C_2H_4) (**5**)	2.112(3), 2.092(3)	1.410(5)	3.00 (-2.25)[c,d]	56.9 (-66.0)[b,d]
BECCIX	κ^2-[PhB(3-C_2F_5-Pz)$_3$]Au(C_2H_4) (**6**)	2.089(8), 2.105(7)	1.366(12)	2.89 (-2.51)[a]	59.3 (-63.8)[a]
FARTOL	κ^2-[(4-*t*-BuC_6H_4)B(6-(CF_3)-Py)$_3$]Au(C_2H_4) (**7**)	2.108(2), 2.104(2)	1.399(4)	2.66 (-2.74)[a]	58.7 (-64.4)[a]
GIBYAV	κ^2-[CH_3B(6-CF_3-Py)$_3$]Au(C_2H_4) (**8**)	2.095(2), 2.1040(19)	1.409(3)	3.41 (-1.99)[a]	57.1 (-65.9)[a]
GIBXIC*	κ^2-[$(CH_3)_2$B(6-CF_3-Py)$_2$]Au(C_2H_4) (**9**)	2.102(10), 2.113(10); 2.091(10), 2.100(10)	1.402(15); 1.377(16)	2.69 (-2.71)[a]	57.6 (-65.5)[a]

RIZYIJ	[1,5-(2,6-$(Cl)_2$-$C_6H_3)_2$-2,4-(*n*-$C_3F_7)_2$TAP]Au(C_2H_4) (**10**)	2.089(2), 2.098(2)	1.405(4)	2.71 (-2.69)[a]	59.1 (-64.0)[a]
KISVOY[†]	[Au($C_2H_4)_3$][SbF_6] (**11**)	2.263(4)-2.272(4); av. 2.268	1.351(7)-1.371(7); av. 1.364	4.94 (-0.46)[b]	92.7 (-30.5)[b]
ZETNUJ*,[†]	[Au($C_2H_4)_3$][Al($OC(CF_3)_3)_4$] (**12**)	2.282(6)-2.323(6); av. 2.306	1.331(10)-1.360(9); av. 1.345	5.35 (-0.05)[b]	104.0 (-19.2)[b]
NICHIT	[(5,5'-$(F)_2$-2,2'-Bipy)Au(C_2H_4)][NTf_2] (**13**)	2.086(3), 2.092(3)	1.399(5)	3.93 (-1.47)[b]	63.8 (-59.4)[b]
XAVWAW	[(4,4'-$(Br)_2$-2,2'-Bipy)Au(C_2H_4)][NTf_2] (**14)**	2.071(6), 2.099(6)	1.397(10)	3.90 (-1.50)[b]	63.6 (-59.6)[b]
XAVWEA	[(4,4'-$(CO_2Me)_2$-2,2'-Bipy)Au(C_2H_4)][NTf_2] (**15**)	2.092(2), 2.092(2)	1.408(5)	3.69 (-1.71)[b]	64.4 (-58.8)[b]
XAVWOK*	[(4,4'-$(CF_3)_2$-2,2'-Bipy)Au(C_2H_4)][NTf_2] (**16**)	2.087(8) 2.098(8); 2.087(9), 2.093(9)	1.413(14); 1.410(16)	4.05 (-1.35)[b]	65.7 (-57.5)[b]
KAMJOB*	[(4,4'-$(OMe)_2$-2,2'-Bipy)Au(C_2H_4)][NTf_2] (**17**)	2.083(3), 2.095(4); 2.075(3), 2.095(3)	1.413(6); 1.408(5)	3.69 (-1.71)[b]	60.3 (-62.9)[b]
ROFQOV*	[(2,9-(*n*-butyl)$_2$-1,10-Phen)Au(C_2H_4)][NTf_2] (**18**)	2.086(6), 2.096(7); 2.104(7), 2.106(7)	1.383(8); 1.411(10)	3.88 (-1.52)[b]	60.6 (-62.6)[b]
OWEYOG	[(*N,N*'-(8-(3,5-$(Cl)_2$-C_6H_3)-1-Nt)butane-2,3-diimine)Au(C_2H_4)][SbF_6] (**19**)	2.094(8), 2.118(8)	1.455(13)	3.30 (-2.10), 3.27 (-2.13)[a,f]	65.4 (-57.7)[a]
HAYYEP	[(H_2C(3,5-$(CH_3)_2$-Pz)$_2$)Au(C_2H_4)][SbF_6] (**20**)	2.098(2), 2.094(2)	1.401(3)	3.60 (-1.80)[b,e]	58.0 (-65.2)[b,e]
GUCBAK	[1-(NMe_2)-2-(P(1-Ad)$_2$))Au(C_2H_4)][SbF_6] (**21**)	2.149(3), 2.141(3)	1.387(5)	4.10 (-1.30)[b]	75.1 (-48.1)[b]

GUCBUE	[(1,2-(PPh_2)$_2$-1,2-dicarborane)Au(C_2H_4)][SbF_6] (**22**)	2.176(9), 2.175(10)	1.365(15)	4.47 (-0.93)[b]	74.0 (-49.2)[b]
ACADOB*	[((2-(4-*t*-BuC_6H_4)-5-*t*-Bu-1-C_6H_3)$_3$P)Au(C_2H_4)][SbF_6] (**23**)	2.218(8), 2.197(8); 2.214(8), 2.197(7)	1.082(14); 1.119(13)	3.79 (-1.61), 3.66 (-1.74)[b,f]	110.0 (-13.2)[b]
ACACOA	[((2-(4-*t*-BuC_6H_4)-5-*t*-Bu-1-C_6H_3)$_3$P)Au(C_2H_4)]$_2$[μ-Ag(C_2H_4)(μ-H_2O)]$_2$[SbF_6]$_4$ (**23a**)	2.216(6), 2.235(6)	1.263(10)		
SILDOK*	[((*t*-Bu)$_2$P(2-(2,4,6-(*i*-Pr)$_3$-C_6H_2)-C_6H_4))Au(C_2H_4)][SbF_6] (**24**)	2.201(13), 2.257(12); 2.237(9), 2.261(9)	1.28(2); 1.353(15)	4.95 (-0.45)[b]	110.9 (-12.3)[b]
SILSEP	[((Cy)$_2$P(2,6-(3,5-(*t*-Bu)$_2$-C_6H_3)-C_6H_3))Au(C_2H_4)][SbF_6] (**25**)	2.210(7), 2.227(7)	1.384(10)	4.77 (-0.63)[b]	109 (-14.2)[b]

As the gold(I)-ethylene interaction is dominated by electrostatic interactions and involves σ-donation and π-backdonation components, the most useful metric for comparing complexes is the ^{13}C NMR chemical shift, specifically the change in chemical shift for ethylene ($\Delta\delta = \delta_{bound} - \delta_{free}$) which will help account for differences in which NMR solvent was used. The C=C bond length and ^{1}H NMR data are useful as well but sometimes suffer from disordered ethylene units, uncertainties resulting from relatively high esd values, and libration effects[71, 114, 140] for the former and ring current effects (*i.e.*, due to flanking aryl group(s)) for the latter. Note that the ethylene C=C bond distance expected should be longer than that of the free ethylene (*cf.*, 1.3369(10) Å from electron diffraction data,[138] 1.3305(10) Å from equilibrium structure utilizing rotational spectroscopic data,[141] and 1.313 Å from X-ray crystallography)[142] in gold adducts involving ethylene→Au σ-donation and Au→ethylene π-backdonation, as they result in the electron density depletion in the ethylene bonding molecular orbitals and increase in the anti-bonding molecular orbitals, respectively.

Table 1 summarizes some structural and spectroscopic features of structurally authenticated gold(I) ethylene complexes. Analysis of the metrical parameters of the $Au(C_2H_4)$ moiety may be analyzed for the various categories of compounds. The cationic, three-coordinate, homoleptic $[Au(C_2H_4)_3][SbF_6]$ (**11**) and $[Au(C_2H_4)_3][Al(OC(CF_3)_3)_4]$ (**12**) show average Au-C distances of 2.296 Å and C=C distances of 1.350 Å. Two coordinate and cationic gold ethylene complexes **23-25** supported by bulky phosphines show the next longest Au-C distances of 2.217 Å (average). Interestingly, the three coordinate, gold(I)-ethylene complex with softer phosphine donors or the mixed P/N ligand (**22** and **21**, respectively) shows relatively long Au-C distances (ranging from 2.141 to 2.176 Å) in comparison to the three coordinate complexes

supported by nitrogen-donors. The latter group shows an average Au-C distance of 2.096 Å (and range from 2.071 to 2.118 Å). Although still few in number, three-coordinate complexes supported by nitrogen donors represent the largest set among gold-ethylene complexes with structural data in the literature, represented by 18 of the 25 complexes. Data also show that in general, there is no notable difference in Au-C bond lengths between the cationic and neutral species of this category. The average C=C distance and ∠C-Au-C angle of these compounds are 1.402 Å and 39.0˚ , respectively.

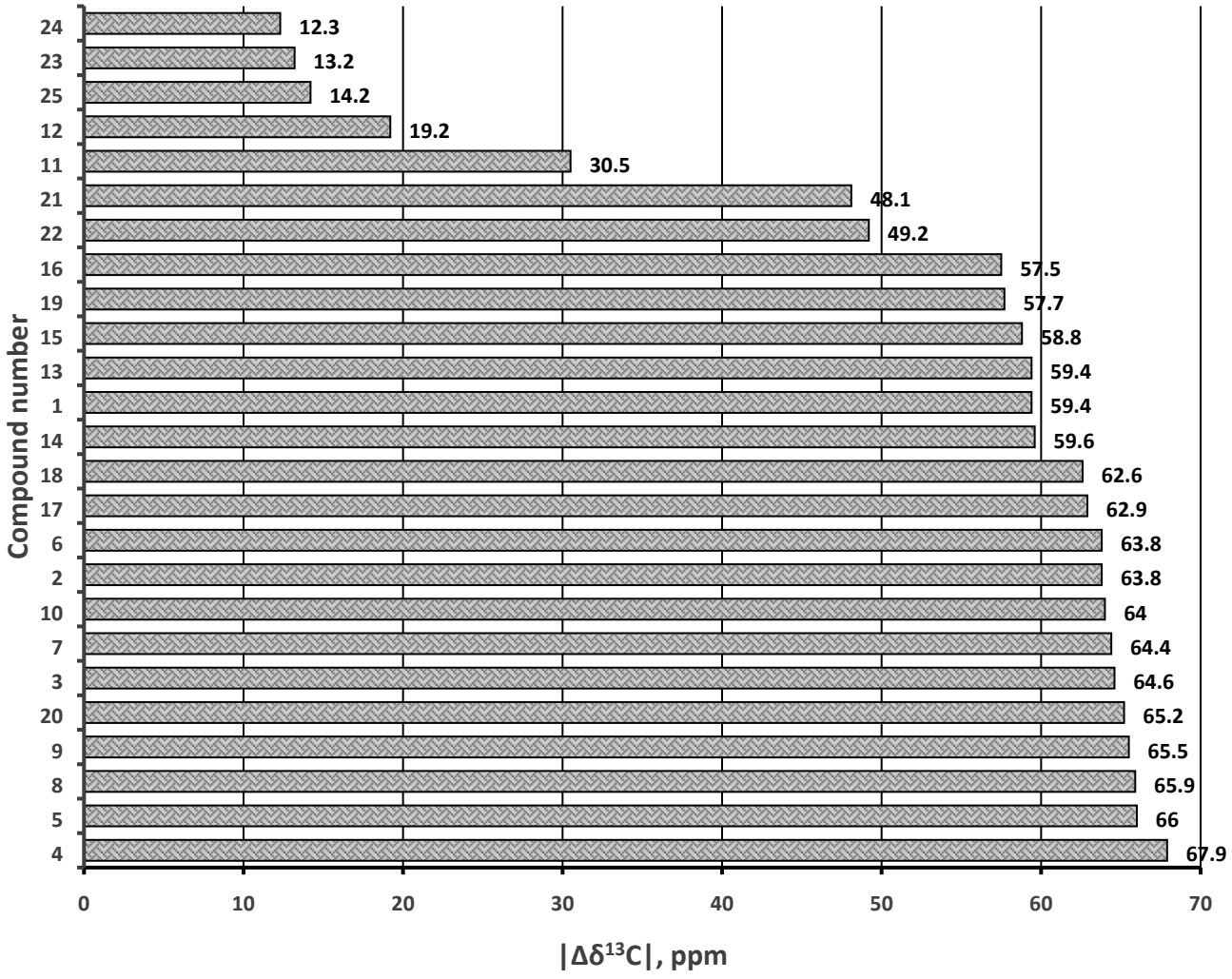

Figure 21. Change in ^{13}C chemical shift relative to free ethylene ($|\Delta\delta^{13}C|$, ppm) for structurally characterized gold-ethylene complexes.

The ^{13}C NMR chemical shift of the gold bound ethylene carbons relative to that of the free ethylene signal (typically observed at δ 122-124 ppm in various NMR solvents)[143] is quite useful in the study of these molecules. By plotting compound numbers *vs.* the change in ^{13}C chemical shift of bound ethylene, several trends emerge (Figure 21). The linear phosphine complexes (**23**–**25**, as well as others from the same references which were not characterized by X-ray crystallography) have the slightest change, ranging from 12.3 to 14.2 ppm, which is even less than the homoleptic tris(ethylene) complexes (**11**, **12**). The other cationic complexes (**13**–**22**) are clustered towards the lower end for the change in chemical shift, with the exception of the electron-donating **20**, whereas the neutral complexes (**1**–**10**) have larger changes in their chemical shift, and thus greater π-backdonation than the cationic complexes, with the exception of the highly electron-deficient complex **1**. When comparing isostructural series such as the κ^2 coordinated tris(pyrazolyl)borates (**1**–**6**) the more electron-donating ligands display the largest shift (*i.e.,* **4**, **5** with upfield shifts of 67.9 and 66.0 ppm respectively), and the most electron-withdrawing ligand **1** displaying the least upfield shift of 59.4 ppm, with the complexes bearing both electron-withdrawing -CF_3 groups and electron-donating -Ph (**2**) and -CH_3 (**3**) groups displaying intermediate upfield shifts of 63.8 and 64.6 ppm, respectively, of the ethylene carbon resonance in ^{13}C NMR (Table 1, Figure 21) from that of the free ethylene signal. This is also observed in the cationic 2,2'-bipyridine and 1,10-phenanthroline series (**13**–**18**). The complexes supported by poly(pyridyl)borate ligands (**7**–**9**) display comparably large upfield shifts between 64.4 and 65.9 ppm, despite bearing electron-withdrawing trifluoromethyl groups on the pyridyl moieties, which can be accredited to poly(pyridyl)borate ligands being relatively better donors than the similar poly(pyrazolyl)borate ligands.[102] The cationic complexes supported by bidentate

phosphine-based ligands **21** and **22** display smaller ethylene group coordination shifts of 48.1 and 49.1 ppm, respectively, when compared to those supported by nitrogen-based ligands which range from 57.5 to 67.9 ppm, possibly due to phosphorous being a softer donor than nitrogen.[144] The complexes supported by monodentate phosphines (**23**–**25**) display the smallest upfield shifts ranging from 12.3 to 14.2 ppm, and therefore the least π-backdonation. The trends in ^{1}H chemical shift are similar to the trends observed in ^{13}C chemical shifts, with the exceptions of molecules with olefinic protons which are heavily influenced by aromatic ring current (*i.e.*, **6**–**8**, **10**, **19**, **23**–**25**).

Vibrational spectroscopy is a useful probe for gauging metal-olefin interactions, based on the variation in C=C stretching frequencies. However, the IR band corresponding to the C=C stretching is very weak and difficult to detect, which is unfortunate as IR is much more widely available and commonly used tool than the Raman spectroscopy. As such, Raman data is only available for six of the structurally authenticated complexes (**11**, **13**–**17**). For free ethylene, the C=C stretch couples heavily with CH_2 scissoring, which produces modes at 1623 cm^{-1} and 1342 cm^{-1},[145] and this mixing is believed to be even larger for metal-ethylene complexes.[146, 147] Therefore, the C=C stretching frequencies should be treated with caution, and ideally be used to support trends coupled with ^{1}H, ^{13}C, and X-ray and computational data. The largest redshift amongst the gold(I)-ethylene complexes was observed with the electron-donating complex **17**, with a value of 1462 cm^{-1} (161 cm^{-1} from free ethylene), and the smallest red-shift was observed with the electron-withdrawing complex **13**, with a value of 1585 cm^{-1} (38 cm^{-1} from free ethylene). The gold(I)-tris(ethylene) complex **11** is reported to have an intermediate value of 1543 cm^{-1} (80 cm^{-1} from free ethylene). It is reasonable to expect that ^{13}C–^{1}H coupled NMR would

serve as a useful probe for the extent of π-backdonation or the amount of *s*-character in the C_{sp2}-H bond. However, there is very little variance in the few complexes which report this value (for **1**, **2**, and **6** $^1J_{C-H}$ is 165 Hz, for **9** and **10** $^1J_{C-H}$ is 162 Hz), the $^1J_{C-H}$ value for free ethylene is 156 Hz.[71]

Summary and Concluding Remarks

In the past 15 years, the number of structurally authenticated gold(I) ethylene complexes has grown significantly beyond just an isolated exotic species. Even more notably, gold has been found extremely useful in numerous applications in homogeneous and heterogeneous catalytic transformations of unsaturated hydrocarbons. The majority of structurally characterized gold(I)-ethylene complexes in the literature feature trigonal planar gold sites, with the recent exception of linear complexes supported by bulky mono-dentate phosphines. Studies have shown that the gold(I)-ethylene interaction is dominated by electrostatic interactions, with significant π-backdonation and σ-acceptance components, and that the extent of π-backdonation can readily be tuned by adjusting the nature of the supporting ligand. Linear, cationic gold complexes supported by phosphines seem to be somewhat unusual, showing minimal π-backdonation. Although gold(III) is also known to form ethylene complexes as demonstrated by Savjani *et al.*,[13, 148] thus far no X-ray structural data are available for such a species. Overall, considering the importance and impact of gold-alkenes, we are optimistic at the continued growth and expansion of gold(I) and gold(III) chemistry, and the isolation of complexes in the future, previously considered unattainable.

Acknowledgements

We acknowledge the support from National Science Foundation under grant number (CHE-1954456, HVRD).

References:

1. G. C. Bond, *Gold Bull.*, 1972, **5**, 11-13.
2. A. S. K. Hashmi, *Gold Bull.*, 2004, **37**, 51-65.
3. G. Bond, *Gold Bull.*, 2008, **41**, 235-241.
4. A. S. K. Hashmi and G. J. Hutchings, *Angew. Chem. Int. Ed.*, 2006, **45**, 7896-7936.
5. A. S. K. Hashmi, *Chem. Rev.*, 2007, **107**, 3180-3211.
6. R. Ciriminna, E. Falletta, C. Della Pina, J. H. Teles and M. Pagliaro, *Angew. Chem. Int. Ed.*, 2016, **55**, 14210-14217.
7. Z. Li, C. Brouwer and C. He, *Chem. Rev.*, 2008, **108**, 3239-3265.
8. D. J. Gorin and F. D. Toste, *Nature*, 2007, **446**, 395-403.
9. A. Fürstner and P. W. Davies, *Angew. Chem. Int. Ed.*, 2007, **46**, 3410-3449.
10. E. Jiménez-Núñez and A. M. Echavarren, *Chem. Commun.*, 2007, 333-346.
11. A. M. Echavarren, A. S. K. Hashmi and F. D. Toste, *Adv. Synth. Catal.*, 2016, **358**, 1347-1347.
12. B. K. Min and C. M. Friend, *Chem. Rev.*, 2007, **107**, 2709-2724.
13. L. Rocchigiani and M. Bochmann, *Chem. Rev.*, 2021, **121**, 8364-8451.
14. J. C. Fierro-Gonzalez and B. C. Gates, *Chem. Soc. Rev.*, 2008, **37**, 2127-2134.
15. M. Navarro and D. Bourissou, in *Adv. Organomet. Chem.*, ed. P. J. Pérez, Academic Press, 2021, vol. 76, pp. 101-144.
16. M. Haruta, *Catal. Today*, 1997, **36**, 153-166.
17. M.-C. Daniel and D. Astruc, *Chem. Rev.*, 2004, **104**, 293-346.
18. K. Sennewald, W. Vogt and H. Glaser, *Patent DE1244766B*, 1967, **20**.
19. G. C. Bond and P. A. Sermon, *Gold Bull.*, 1973, **6**, 102-105.
20. G. C. Bond, *Gold Bull.*, 2016, **49**, 53-61.
21. G. J. Hutchings, *J. Catal.*, 1985, **96**, 292-295.
22. M. Haruta, T. Kobayashi, H. Sano and N. Yamada, *Chem. Lett.*, 1987, **16**, 405-408.
23. M. Haruta, *Nature*, 2005, **437**, 1098-1099.
24. G. J. Hutchings, *Catal. Today*, 2005, **100**, 55-61.
25. G. J. Hutchings, M. Brust and H. Schmidbaur, *Chem. Soc. Rev.*, 2008, **37**, 1759-1765.
26. T. Hayashi, K. Tanaka and M. Haruta, *J. Catal.*, 1998, **178**, 566-575.
27. J. Huang, T. Akita, J. Faye, T. Fujitani, T. Takei and M. Haruta, *Angew. Chem. Int. Ed.*, 2009, **48**, 7862-7866.
28. N. Kapil, T. Weissenberger, F. Cardinale, P. Trogadas, T. A. Nijhuis, M. M. Nigra and M.-O. Coppens, *Angew. Chem. Int. Ed.*, 2021, **60**, 18185-18193.
29. A. K. Sinha, S. Seelan, S. Tsubota and M. Haruta, *Top. Catal.*, 2004, **29**, 95-102.
30. J. Guzman and B. C. Gates, *Angew. Chem. Int. Ed.*, 2003, **42**, 690-693.
31. J. Guzman and B. C. Gates, *J. Catal.*, 2004, **226**, 111-119.
32. Y. Ito, M. Sawamura and T. Hayashi, *J. Am. Chem. Soc.*, 1986, **108**, 6405-6406.

33. J. H. Teles, S. Brode and M. Chabanas, *Angew. Chem. Int. Ed.*, 1998, **37**, 1415-1418.
34. E. Mizushima, K. Sato, T. Hayashi and M. Tanaka, *Angew. Chem. Int. Ed.*, 2002, **41**, 4563-4565.
35. A. S. K. Hashmi, T. M. Frost and J. W. Bats, *J. Am. Chem. Soc.*, 2000, **122**, 11553-11554.
36. A. S. K. Hashmi, L. Schwarz, J.-H. Choi and T. M. Frost, *Angew. Chem. Int. Ed.*, 2000, **39**, 2285-2288.
37. S. Kobayashi, K. Kakumoto and M. Sugiura, *Org. Lett.*, 2002, **4**, 1319-1322.
38. M. J. Johansson, D. J. Gorin, S. T. Staben and F. D. Toste, *J. Am. Chem. Soc.*, 2005, **127**, 18002-18003.
39. X.-Y. Liu, C.-H. Li and C.-M. Che, *Org. Lett.*, 2006, **8**, 2707-2710.
40. J. Zhang, C.-G. Yang and C. He, *J. Am. Chem. Soc.*, 2006, **128**, 1798-1799.
41. C.-G. Yang and C. He, *J. Am. Chem. Soc.*, 2005, **127**, 6966-6967.
42. M. A. Cinellu, G. Minghetti, F. Cocco, S. Stoccoro, A. Zucca and M. Manassero, *Angew. Chem. Int. Ed.*, 2005, **44**, 6892-6895.
43. M. A. Cinellu, G. Minghetti, F. Cocco, S. Stoccoro, A. Zucca, M. Manassero and M. Arca, *Dalton Trans.*, 2006, 5703-5716.
44. J. A. Flores and H. V. R. Dias, *Inorg. Chem.*, 2008, **47**, 4448-4450.
45. E. Langseth, A. Nova, E. A. Tråseth, F. Rise, S. Øien, R. H. Heyn and M. Tilset, *J. Am. Chem. Soc.*, 2014, **136**, 10104-10115.
46. S. G. Rull, A. Olmos and P. J. Pérez, *Beilstein J. Org. Chem.*, 2019, **15**, 67-71.
47. Z. Zhang, S. D. Lee and R. A. Widenhoefer, *J. Am. Chem. Soc.*, 2009, **131**, 5372-5373.
48. M. J. Harper, E. J. Emmett, J. F. Bower and C. A. Russell, *J. Am. Chem. Soc.*, 2017, **139**, 12386-12389.
49. M. Lin, H. Wang, T. Takei, H. Miura, T. Shishido, Y. Li, J. Hu, Y. Inomata, T. Ishida, M. Haruta, G. Xiu and T. Murayama, *Nat. Commun.*, 2023, **14**, 2885.
50. S. C. Scott, J. A. Cadge, G. K. Boden, J. F. Bower and C. A. Russell, *Angew. Chem. Int. Ed.*, 2023, **62**, e202301526.
51. M. Livendahl, C. Goehry, F. Maseras and A. M. Echavarren, *Chem. Commun.*, 2014, **50**, 1533-1536.
52. I. Fernández, L. P. Wolters and F. M. Bickelhaupt, *J. Comput. Chem.*, 2014, **35**, 2140-2145.
53. S. G. Bratsch, *Journal of Physical and Chemical Reference Data*, 1989, **18**, 1-21.
54. T. Lauterbach, M. Livendahl, A. Rosellón, P. Espinet and A. M. Echavarren, *Org. Lett.*, 2010, **12**, 3006-3009.
55. P. S. D. Robinson, G. N. Khairallah, G. da Silva, H. Lioe and R. A. J. O'Hair, *Angew. Chem. Int. Ed.*, 2012, **51**, 3812-3817.
56. L. T. Ball, G. C. Lloyd-Jones and C. A. Russell, *Science*, 2012, **337**, 1644-1648.
57. L. T. Ball, G. C. Lloyd-Jones and C. A. Russell, *J. Am. Chem. Soc.*, 2014, **136**, 254-264.
58. B. Sahoo, M. N. Hopkinson and F. Glorius, *J. Am. Chem. Soc.*, 2013, **135**, 5505-5508.
59. M. N. Hopkinson, B. Sahoo and F. Glorius, *Adv. Synth. Catal.*, 2014, **356**, 2794-2800.
60. V. Gauchot and A.-L. Lee, *Chem. Commun.*, 2016, **52**, 10163-10166.
61. V. Gauchot, D. R. Sutherland and A. L. Lee, *Chem. Sci.*, 2017, **8**, 2885-2889.
62. B. Dong, H. Peng, S. E. Motika and X. Shi, *Chem. - Eur. J.*, 2017, **23**, 11093-11099.
63. J. Xie, K. Sekine, S. Witzel, P. Krämer, M. Rudolph, F. Rominger and A. S. K. Hashmi, *Angew. Chem. Int. Ed.*, 2018, **57**, 16648-16653.
64. S. Witzel, K. Sekine, M. Rudolph and A. S. K. Hashmi, *Chem. Commun.*, 2018, **54**, 13802-13804.
65. M. Joost, A. Zeineddine, L. Estévez, S. Mallet–Ladeira, K. Miqueu, A. Amgoune and D. Bourissou, *J. Am. Chem. Soc.*, 2014, **136**, 14654-14657.
66. A. Zeineddine, L. Estévez, S. Mallet-Ladeira, K. Miqueu, A. Amgoune and D. Bourissou, *Nat. Commun.*, 2017, **8**, 565.

67. S. Dutta, *Energy Fuels*, 2023, **37**, 2648-2666.
68. Y. Gao, L. Neal, D. Ding, W. Wu, C. Baroi, A. M. Gaffney and F. Li, *ACS Catal.*, 2019, **9**, 8592-8621.
69. A. S. K. Hashmi, *Angew. Chem. Int. Ed.*, 2010, **49**, 5232-5241.
70. S. M. Lang, T. M. Bernhardt, J. M. Bakker, B. Yoon and U. Landman, *J. Condens. Matter Phys.*, 2018, **30**, 504001.
71. H. V. R. Dias and J. Wu, *Eur. J. Inorg. Chem.*, 2008, 509-522.
72. H. V. R. Dias and J. Wu, *Eur. J. Inorg. Chem.*, 2008, 2113-2113.
73. C. R. Groom, I. J. Bruno, M. P. Lightfoot and S. C. Ward, *Acta Cryst. B*, 2016, **72**, 171-179.
74. J. Dewar, *Bull. Soc. chim. Fr.*, 1951, **18**, C71-C79.
75. J. Chatt and L. A. Duncanson, *J. Chem. Soc.*, 1953, 2939-2947.
76. R. H. Hertwig, W. Koch, D. Schröder, H. Schwarz, J. Hrušák and P. Schwerdtfeger, *J. Phys. Chem.*, 1996, **100**, 12253-12260.
77. T. Ziegler and A. Rauk, *Inorg. Chem.*, 1979, **18**, 1558-1565.
78. M. S. Nechaev, V. M. Rayón and G. Frenking, *J. Phys. Chem. A*, 2004, **108**, 3134-3142.
79. N. J. Barnett, L. V. Slipchenko and M. S. Gordon, *J. Phys. Chem. A*, 2009, **113**, 7474-7481.
80. J. T. York, *J. Phys. Chem. A*, 2016, **120**, 6064-6075.
81. H. V. R. Dias and C. J. Lovely, *Chem. Rev.*, 2008, **108**, 3223-3238.
82. A. Muñoz-Castro and H. V. R. Dias, *J. Comput. Chem.*, 2022, **43**, 1848-1855.
83. J. Wu, A. Noonikara-Poyil, A. Muñoz-Castro and H. V. R. Dias, *Chem. Commun.*, 2021, **57**, 978-981.
84. M. Vanga, A. Muñoz-Castro and H. V. R. Dias, *Dalton Trans.*, 2022, **51**, 1308-1312.
85. J. Forniés, A. Martín, L. F. Martín, B. Menjón and A. Tsipis, *Organometallics*, 2005, **24**, 3539-3546.
86. J. Mehara, B. T. Watson, A. Noonikara-Poyil, A. O. Zacharias, J. Roithová and H. V. Rasika Dias, *Chem. - Eur. J.*, 2022, **28**, e202103984.
87. H. V. R. Dias and J. Wu, *Angew. Chem. Int. Ed.*, 2007, **46**, 7814-7816.
88. S. Alvarez, *Dalton Trans.*, 2013, **42**, 8617-8636.
89. A. Bondi, *J. Phys. Chem.*, 1964, **68**, 441-451.
90. T. A. Albright, R. Hoffmann, J. C. Thibeault and D. L. Thorn, *J. Am. Chem. Soc.*, 1979, **101**, 3801-3812.
91. N. Rosch and R. Hoffmann, *Inorg. Chem.*, 1974, **13**, 2656-2666.
92. R. M. Pitzer and H. F. Schaefer, III, *J. Am. Chem. Soc.*, 1979, **101**, 7176-7183.
93. S. G. Ridlen, J. Wu, N. V. Kulkarni and H. V. R. Dias, *Eur. J. Inorg. Chem.*, 2016, **2016**, 2573-2580.
94. H. V. R. Dias and J. Wu, *Organometallics*, 2012, **31**, 1511-1517.
95. M. Vanga, V. Q. H. Phan, J. Wu, A. Muñoz-Castro and H. V. R. Dias, *Inorg. Chem.*, 2023, **62**, 18563-18572.
96. M. Vanga, A. Noonikara-Poyil, J. Wu and H. V. R. Dias, *Organometallics*, 2022, **41**, 1249-1260.
97. C. Cui, R. A. Lalancette and F. Jäkle, *Chem. Commun.*, 2012, **48**, 6930-6932.
98. C. Cui, P. R. Shipman, R. A. Lalancette and F. Jäkle, *Inorg. Chem.*, 2013, **52**, 9440-9448.
99. P. O. Shipman, C. Cui, P. Lupinska, R. A. Lalancette, J. B. Sheridan and F. Jäkle, *ACS Macro Lett.*, 2013, **2**, 1056-1060.
100. G. M. Pawar, R. A. Lalancette, E. M. Bonder, J. B. Sheridan and F. Jäkle, *Macromolecules*, 2015, **48**, 6508-6515.
101. S. Y. Jeong, R. A. Lalancette, H. Lin, P. Lupinska, P. O. Shipman, A. John, J. B. Sheridan and F. Jäkle, *Inorg. Chem.*, 2016, **55**, 3605-3615.
102. G. M. Pawar, J. B. Sheridan and F. Jäkle, *Eur. J. Inorg. Chem.*, 2016, **2016**, 2227-2235.
103. J. Qian and R. J. Comito, *Organometallics*, 2021, **40**, 1817-1821.

104. B. T. Watson, M. Vanga, A. Noonikara-Poyil, A. Muñoz-Castro and H. V. R. Dias, *Inorg. Chem.*, 2023, **62**, 1636-1648.
105. M. K. Pennington-Boggio, B. L. Conley, M. G. Richmond and T. J. Williams, *Polyhedron*, 2014, **84**, 24-31.
106. H. V. R. Dias and S. Singh, *Inorg. Chem.*, 2004, **43**, 7396-7402.
107. H. V. R. Dias, M. Fianchini, T. R. Cundari and C. F. Campana, *Angew. Chem. Int. Ed.*, 2008, **47**, 556-559.
108. K. Fischer, K. Jonas and G. Wilke, *Angew. Chem., Int. Ed. Engl.*, 1973, **12**, 565-566.
109. N. Hebben, H. J. Himmel, G. Eickerling, C. Herrmann, M. Reiher, V. Herz, M. Presnitz and W. Scherer, *Chemistry*, 2007, **13**, 10078-10087.
110. A. P. Rainer Herges, *Angew. Chem.*, 2001, **113**, 4809-4813.
111. M. Fianchini, C. F. Campana, B. Chilukuri, T. R. Cundari, V. Petricek and H. V. R. Dias, *Organometallics*, 2013, **32**, 3034-3041.
112. J. Schaefer, D. Himmel and I. Krossing, *Eur. J. Inorg. Chem.*, 2013, **2013**, 2712-2717.
113. G. Santiso-Quiñones, A. Reisinger, J. Slattery and I. Krossing, *Chem. Commun.*, 2007, 5046-5048.
114. A. Reisinger, N. Trapp, C. Knapp, D. Himmel, F. Breher, H. Rüegger and I. Krossing, *Chem. - Eur. J.*, 2009, **15**, 9505-9520.
115. M. J. Harper, C. J. Arthur, J. Crosby, E. J. Emmett, R. L. Falconer, A. J. Fensham-Smith, P. J. Gates, T. Leman, J. E. McGrady, J. F. Bower and C. A. Russell, *J. Am. Chem. Soc.*, 2018, **140**, 4440-4445.
116. J. A. Cadge, J. F. Bower and C. A. Russell, *Angew. Chem. Int. Ed.*, 2021, **60**, 24976-24983.
117. C. Amatore, E. Carre, A. Jutand and M. A. M'Barki, *Organometallics*, 1995, **14**, 1818-1826.
118. Y. Yang, P. Antoni, M. Zimmer, K. Sekine, F. F. Mulks, L. Hu, L. Zhang, M. Rudolph, F. Rominger and A. S. K. Hashmi, *Angew. Chem. Int. Ed.*, 2019, **58**, 5129-5133.
119. D. Whitaker, J. Burés and I. Larrosa, *J. Am. Chem. Soc.*, 2016, **138**, 8384-8387.
120. M. D. Lotz, N. M. Camasso, A. J. Canty and M. S. Sanford, *Organometallics*, 2017, **36**, 165-171.
121. A. Fattahi, R. E. McCarthy, M. R. Ahmad and S. R. Kass, *J. Am. Chem. Soc.*, 2003, **125**, 11746-11750.
122. S. Y. Lee and J. F. Hartwig, *J. Am. Chem. Soc.*, 2016, **138**, 15278-15284.
123. K. Klimovica, K. Kirschbaum and O. Daugulis, *Organometallics*, 2016, **35**, 2938-2943.
124. E. T. Nadres, G. I. F. Santos, D. Shabashov and O. Daugulis, *J. Org. Chem.*, 2013, **78**, 9689-9714.
125. J. Rodriguez, A. Zeineddine, E. D. Sosa Carrizo, K. Miqueu, N. Saffon-Merceron, A. Amgoune and D. Bourissou, *Chem. Sci.*, 2019, **10**, 7183-7192.
126. M. Navarro, A. Toledo, S. Mallet-Ladeira, E. D. Sosa Carrizo, K. Miqueu and D. Bourissou, *Chem. Sci.*, 2020, **11**, 2750-2758.
127. M. Navarro, J. Miranda-Pizarro, J. J. Moreno, C. Navarro-Gilabert, I. Fernández and J. Campos, *Chem. Commun.*, 2021, **57**, 9280-9283.
128. J. Keller, C. Schlierf, C. Nolte, P. Mayer and B. F. Straub, *Synthesis*, 2006, **2006**, 354-365.
129. D. Zuccaccia, L. Belpassi, F. Tarantelli and A. Macchioni, *J. Am. Chem. Soc.*, 2009, **131**, 3170-3171.
130. P. de Frémont, N. Marion and S. P. Nolan, *J. Organomet. Chem.*, 2009, **694**, 551-560.
131. T. J. Brown, M. G. Dickens and R. A. Widenhoefer, *Chem. Commun.*, 2009, 6451-6453.
132. T. N. Hooper, M. Green, J. E. McGrady, J. R. Patel and C. A. Russell, *Chem. Commun.*, 2009, 3877-3879.
133. P. Motloch, J. Blahut, I. Císařová and J. Roithová, *J. Organomet. Chem.*, 2017, **848**, 114-117.
134. C. Griebel, D. D. Hodges, B. R. Yager, F. L. Liu, W. Zhou, K. J. Makaravage, Y. Zhu, S. G. Norman, R. Lan, C. S. Day and A. C. Jones, *Organometallics*, 2020, **39**, 2665-2671.
135. J. Campos, *J. Am. Chem. Soc.*, 2017, **139**, 2944-2947.
136. N. Hidalgo, J. J. Moreno, M. Pérez-Jiménez, C. Maya, J. López-Serrano and J. Campos, *Chem. - Eur. J.*, 2020, **26**, 5982-5993.

137. N. Hidalgo, J. J. Moreno, M. Pérez-Jiménez, C. Maya, J. López-Serrano and J. Campos, *Organometallics*, 2020, **39**, 2534-2544.
138. L. S. Bartell, E. A. Roth, C. D. Hollowell, K. Kuchitsu and J. E. Young, Jr., *J. Chem. Phys.*, 1965, **42**, 2683-2686.
139. M. Navarro, M. G. Alférez, M. de Sousa, J. Miranda-Pizarro and J. Campos, *ACS Catal.*, 2022, **12**, 4227-4241.
140. P. Müller in P. Müller, R. Herbst-Irmer, A. L. Spek, T. R. Schneider and M. R. Sawaya, in *Crystal Structure Refinement: A Crystallographer's Guide to SHELXL*, Oxford University Press, 2006, p 150-158.
141. N. C. Craig, P. Groner and D. C. McKean, *J. Phys. Chem. A*, 2006, **110**, 7461-7469.
142. G. J. H. Nes and A. Vos, *Acta Cryst. B*, 1979, **35**, 2593-2601.
143. G. R. Fulmer, A. J. M. Miller, N. H. Sherden, H. E. Gottlieb, A. Nudelman, B. M. Stoltz, J. E. Bercaw and K. I. Goldberg, *Organometallics*, 2010, **29**, 2176-2179.
144. R. G. Pearson, *J. Am. Chem. Soc.*, 1963, **85**, 3533-3539.
145. E. Maslowsky Jr, *Vibrational spectra of organometallics: theoretical and experimental data*, John Wiley & Sons, 2019, p 355.
146. L. Manceron and L. Andrews, *J. Phys. Chem.*, 1986, **90**, 4514-4528.
147. N. Hebben, H.-J. Himmel, G. Eickerling, C. Herrmann, M. Reiher, V. Herz, M. Presnitz and W. Scherer, *Chem. - Eur. J.*, 2007, **13**, 10078-10087.
148. N. Savjani, D.-A. Roşca, M. Schormann and M. Bochmann, *Angew. Chem. Int. Ed.*, 2013, **52**, 874-877.